5-2007

Studies on a 50S Ribosomal Precursor Particle as a Substrate for *erm* E Methyltransferase Enzyme in *Staphylococcus aureus* .

Indira Pokkunuri
East Tennessee State University

Studies on a 50S Ribosomal Precursor Particle as a Substrate for *erm*E Methyltransferase Enzyme in *Staphylococcus aureus*

A dissertation

presented to

the faculty of the Department of Biochemistry and Molecular Biology

East Tennessee State University

In partial fulfillment

of the requirements for the degree

Doctor of Philosophy in Biomedical Sciences

---

by

Indira Devi Pokkunuri

May 2007

Scott Champney, Chair

David Johnson

John Laffan

Antonio Rusinol

Robert Schoborg

Keywords: 50S precursor particle, *erm*E methyltransferase, MLS_B antibiotics

ABSTRACT

Studies on a 50S Ribosomal Precursor Particle as a Substrate for *erm*E Methyltransferase Enzyme in *Staphylococcus aureus*

by

Indira Pokkunuri

Erythromycin is a macrolide antibiotic that inhibits not only mRNA translation but also 50S ribosomal subunit assembly in bacterial cells. An important mechanism of erythromycin resistance is the methylation of 23S rRNA by *erm* methyl transferase enzymes. We are interested in investigating the true substrate for methylation because it is known from our work and the work of others that fully assembled 50S subunits are not substrates for methylation. We have published a model for 50S ribosomal subunit formation where, the precursor particle that accumulates in erythromycin treated cells is a target for methyl transferase activity. Current studies are aimed at investigating the role of the precursor particle as substrate for *erm*E methyltransferase activity and the competition between this enzyme and erythromycin for the 50S precursor particle.

Slot-blot hybridization experiments have identified the presence of 23S rRNA in the 50S precursor region. Quantitation of the 23S rRNA in these blots also revealed that the percentage of the precursor increased as the concentration of erythromycin was increased in the growth media. Ribosomal proteins of *S. aureus* were studied by two-dimensional gel electrophoresis. Protein content of the 50S precursor particle was

analyzed by MALDI-TOF. These studies have identified 16 50S ribosomal proteins in the precursor region.

Methyltransferase assays showed that 50S precursor particle was a substrate for *erm*E methyltransferase. Importantly, RNA that is already assembled into 50S subunits was not a substrate for the enzyme. Inhibition curves showed that macrolide, lincosamide, and streptogramin B (MLS_B) drugs bound to the precursor particle with similar affinity and inhibited the *erm*E methyltransferase activity. Competition experiments suggested that the enzyme can displace erythromycin from the 50S precursor particle and that *erm* methyltransferase has a lower association constant for the precursor particle compared to that of the erythromycin. This suggests that higher concentrations of erythromycin are needed to combat *erm* induced resistance.

These studies shed light on the interaction of *erm*E methyltransferase and erythromycin in the clinically important pathogen *S. aureus.*

.

ACKNOWLEDGEMENTS

First of all, I must thank God for blessing me with a good life. Then, I would like to thank my wonderful advisor Dr. Scott Champney for his constant encouragement and for always being positive. He has been a source of inspiration for me both as a scientist and as a person. Thank you Dr. Champney for all that you are! Then I would like to thank my most intellectual committee members, Dr. Johnson, Dr. Laffan, Dr. Rusinol, and Dr. Schoborg for their constant guidance and support. I would also like to thank my wonderful labmates and very good friends Cerrone and Susan for always being there for me. I would also like to thank Dr. Robinson for giving me an opportunity to be a part of this program that provided a very amicable atmosphere for me. Then, I would like to thank the three wonderful women, Karen, Ray, and Beverly, who gave me the warmth and comfort of a family!

I would also like to thank my father, my sisters, my brother and all my other family members. I am so proud of my father for the gem of a person he is and I am grateful to him for always providing us the most conducive and encouraging ambience to realize our dreams! I would like to extend my special thanks to Dr. Panini and Dr. Aruna Panini for being always being there for me through thick and thin! I would also like to thank all my loving friends Suman, Dipti, Raj, Rinti, Abhijeet, Amit, and Pranoti, who have given me an enormous emotional support. Last but not the least, I would like to thank my beloved husband Raghav for being so patient and supportive through the ups and downs of my research. You kept the faith in me during the toughest times and provided me constant support. You made this arduous task of Ph.D. possible to achieve. I am privileged to have you in my life!

CONTENTS

LIST OF TABLES

LIST OF FIGURES

CHAPTER 1

INTRODUCTION

For many years, antibiotics have been effective in the treatment of many infectious diseases caused by a range of pathogens, including *Staphylococcus aureus* (Marana et al. 1997). But the continuing increase in antibiotic resistance among bacteria has transformed some previously treatable diseases into new threat to public health (Cohen 1994, Rubinstein 1994, Anderson 1999). The number of resistant bacterial strains keeps increasing and antibiotics are rapidly loosing their efficacy (Amabile-Cuevas 1995, Chu and Katz 1996). Consequently, there is an increasing need for an in- depth understanding of the antibiotic resistance mechanisms in this post-antibiotic era.

Ribosomes are the primary target for a majority of antibiotics (Marana et al. 1997). Ribosomes are sophisticated molecular machines to ensure that the genetic information is reliably translated into proteins (Liebold 1986, Garrett et al. 2000). The structure of the ribosome reflects its functional complexity. In bacteria, ribosomes consist of two ribonucleoprotein complexes, the small 30S subunit and the large 50S subunit. The 30S subunit is made up of 16S rRNA and 21 proteins, whereas the large 50S subunit consists of 5S and 23S rRNA and 36 proteins.

S. aureus is a ubiquitous bacterium that causes infections in all age groups. *Staphylococci* are non-spore-forming Gram-positive bacteria that belong to the Micrococcaceae family. It is a major causative agent in surgical wound infections and other systemic infections like osteomyelitis, endocarditis, pneumonia, and septicemia

(Cohen and Quinn 1982). A variety of clinical syndromes are associated with genetic elements harbored by *S. aureus* strains like RN -3985 and NZ-39 that encode certain toxins (Meissner et.al. 1993, Parsonett and Marchette 1994). Examples include staphylococcal food poisoning and toxic shock syndrome. Also, *S. aureus* is the most frequently reported pathogen causing nosocomial infections in infants and children (Cabezudo and Wenzel 1982).

Macrolide antibiotics have been effective in treating the infections caused by *S. aureus*, *Streptococcus,* and other Gram-positive organisms. This class of antibiotics inhibit protein synthesis by binding in a stoichiometric fashion to the peptidyl transferase center (PTC) catalyzing the peptide bond formation in the 50S subunit of the bacterial ribosome (Vazquez 1979, Mazzei et al. 1993, Weisblum 1995). Although ribosomal proteins can affect the binding and action of ribosome-targeted antibiotics, the primary target of these antibiotics is rRNA (Cundliffe 1990). But the therapeutic utility of macrolides has been severely compromised by the emergence of drug resistance in these pathogenic bacteria (Voss and Doebelling 1995).

Macrolides, together with two other related classes of antibiotics, lincosamides and streptogramins B, share overlapping binding sites on the 50S ribosomal subunit. They are together called MLS_B antibiotics (Spahn and Prescott 1996) (Figure 1).

A.

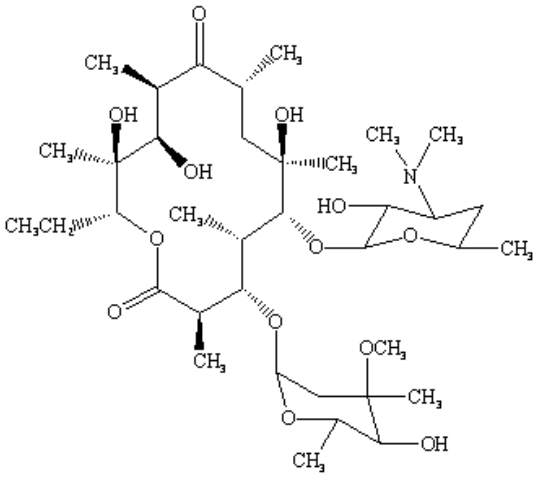

B.

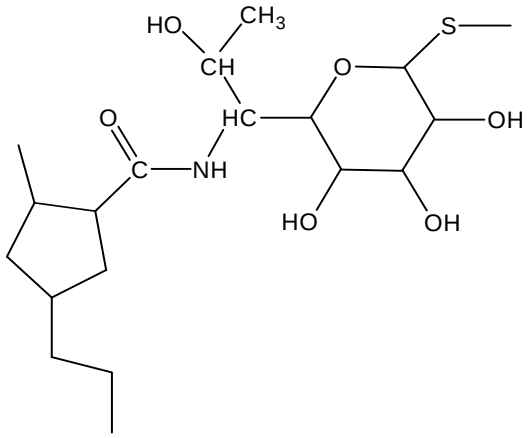

C.

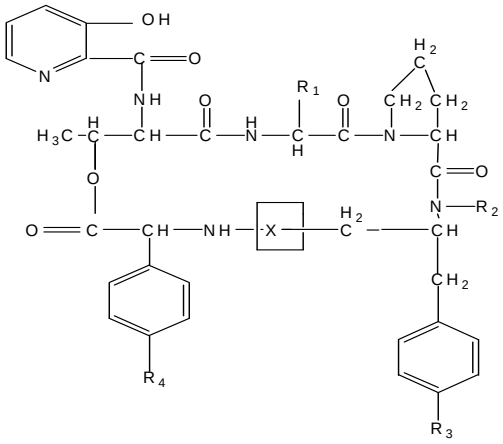

Figure 1 Structure of MLS antibiotics. (A) Erythromycin (Macrolide), (B) Lincomycin (Lincosamide), (C) Virginiamycin S (Streptogramin).

Structure probing studies of 23S rRNA with the antibiotics has revealed similar binding interactions between these compounds (Moazed and Noller 1987, Douthwaite 1992, Kirillov 1999). Within the 23S rRNA, the binding site for MLS antibiotics is composed of domain V sequences near the PTC that serve as a channel for the

growing polypeptide chain (Figure 2). These drugs exhibit competitive binding to the 50S subunits whereby binding of one class of drugs is competed by an excess of another class of drugs (DiGiambattista and Vanuffel 1986). Bacterial cells resistant to one class of antibiotics can show cross-resistance to the other two classes (Leclercq 1991, Leclercq and Courvalin 2002). Resistance to macrolide, lincosamide, and streptogramin B (MLS_B) antibiotics comprises a resistance syndrome of bacteria widely distributed in nature called MLS_B resistance (Duval 1985).

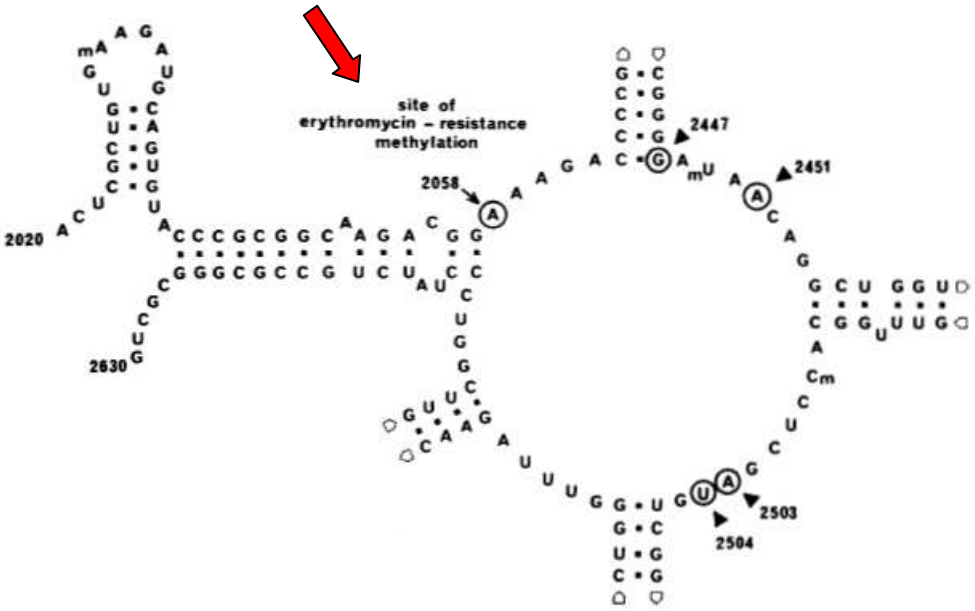

Figure 2 Secondary structure diagram of the peptidyl transferase loop and a loop from domain V of *E. coli* 23S rRNA along with the sequence numbers. Shown in this model is the site of action of erythromycin resistant methylase residue A2058 (Orange arrow).

Inhibition of protein synthesis by macrolides has two distinctive features (Gale 1981, Kirillov 1997). First, macrolides neither bind to nor inhibit the peptide-forming activity (Pestka 1972, Anderson and Kurland 1987) of ribosomes that are

already engaged in protein synthesis. Second, in ribosomes that do not have nascent peptides bound, synthesis stops after the first 5 amino acids (Odom 1991).

Erythromycin is a 14-membered macrolide antibiotic that is effective against a variety of Gram-positive bacteria. Discovered in 1952, it was the first macrolide to enter clinical use, and it remains to this day one of the most widely used macrolides along with many of its derivates. It is produced in an actinomycetes species *Streptomyces erythreus.* As shown in Figure 1 it has a macrolactone ring to which two sugar residues L-Cladinose and D-Desosamine are attached through glycosidic bonds.

The binding site for the macrolides is located on the large ribosomal subunit inside the nascent peptide exit tunnel near the PTC (Figure 3). The reactive groups of the desosamine sugar and the lactone ring mediate all the hydrogen-bond interactions of erythromycin with the PTC. But the shorter desosamine residue of the 14- membered ring macrolides does not reach the peptidyl transferase center, which explains the lack of inhibitory effects of these drugs on the reaction of transpeptidization. The exit tunnel is formed primarily by 23S rRNA. It starts at the PTC and spans the entire body of the subunit finally opening at its back (Bernabeu and Lake 1982, Frank and Zhu 1995, Ban et al. 2000).

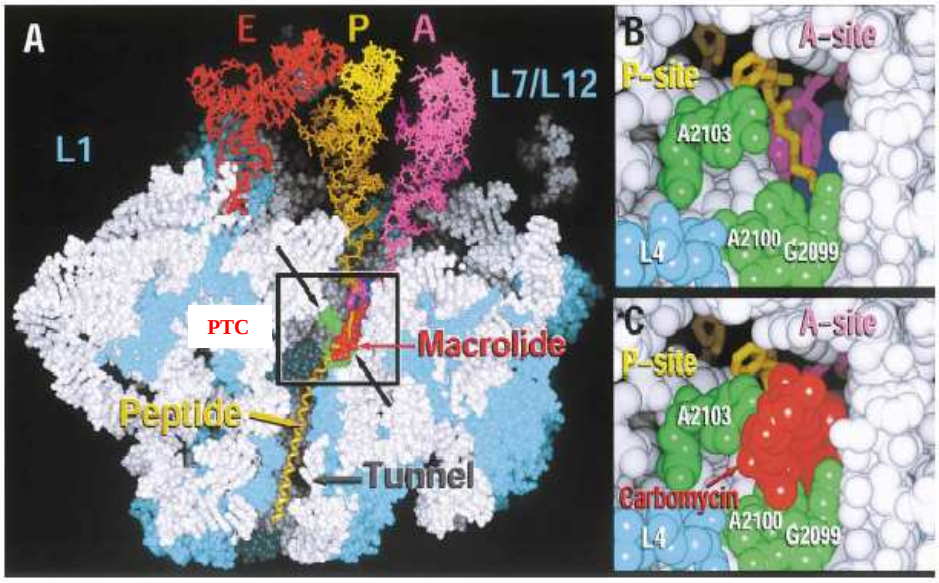

Figure 3 Global views of the macrolide binding site showing how they block the peptide exit tunnel of *Haloarcula marismortui*. (A) Macrolide Binding site: The top of the ribosome is rotated backward from the crown view so that the peptide exit tunnel (gray) with modeled peptide (orange ribbon) can be seen when the front half of the ribosome is removed. Ribosomal RNA is white and ribosomal proteins are light blue space-filling representations. The E-site tRNA (red sticks), A-site tRNA (purple sticks), and P-site tRNA (orange sticks) have been positioned using the coordinates from the 70S ribosome complex after superposition of corresponding 50S subunit atoms. PTC indicates peptidyl transferase center. Black arrows point to an opening between the peptidyl transferase center and the peptide exit tunnel where the macrolides (red) bind. The green atoms are the bases that interact with the macrolides.
(B) Constriction. An alternate view up the exit tunnel, through the constriction, shows P- site (orange sticks) and A-site (purple sticks) substrates bound to the active sites. (C) Blockage. The opening shown in (B) is occluded by both the presence of macrolide (red) and the extended conformation of A 2103 (*E. coli* A2062) (green). Adapted from (Hansen et al. 2002)

Although originally conceived as an inert conduit for any nascent peptides, the tunnel is now considered as an active and dynamic functional entity (Gabashvili and Gregory 2001) that is relatively wide (avg. 150 Å). However, it contains a constriction of 100 Å formed by proteins L4 and L22, which is located at a short distance from PTC. Macrolides bind close to this constriction and pose a molecular road block for the growing peptide chain (Gabashvili and Gregory 2001, Schlunzen and Zarivach 2001, Hansen et al. 2002). In the presence of bound 14 or 15 membered macrolides, polymerization of the first few amino acids proceeds unperturbed. Inhibition of polypeptide growth occurs only after it becomes long enough to reach the bound macrolide near the constriction. Inhibition of peptide elongation eventually results in the dissociation of peptidyl tRNA from the ribosome.

The length of the oligopeptide synthesized in the presence of macrolide antibiotics is determined by the extent to which substituents at position C5 position of the lactone ring penetrate the peptidyl transferase center. Erythromycin, which has a monosaccharide at position C5, permits the synthesis of peptides up to 8 amino acids long before the peptidyl tRNA is dropped off the ribosome.

There are several known mechanisms by which bacteria exhibit resistance to the inhibitory effects of macrolides. These fall into three main classes:
(i) deficiency of macrolide entrance into the cell (Weisblum 1979, Lampson et al.1986), (ii) chemical inactivation of the macrolide (Arthur and Andremont 1987, Wiley 1987), (iii) absence of macrolide binding to the target site (Lai and Weisblum 1971, Duval 1985). The latter mechanism of resistance to MLS_B antibiotics is due to an alteration of their target site (Takashima 2003, Hansen et al 2006,) in the ribosome.

The most frequently occurring mechanism of erythromycin resistance is the target site modification of A2058 by dimethylation (Weisblum 1995). A2058 is an important residue near the PTC for macrolide binding with its N1 and N6 forming two hydrogen bonds with the 2'OH of desosamine sugar of the macrolide. Any modification of this residue would diminish macrolide binding leading to resistance (Figure 2). Organisms that have multiple rRNA cistrons often become resistant by acquiring genes for enzymes that methylate N6 of A2058. This is because in these organisms resistance by point mutation in one gene is compensated by the wild type sequence in another gene whereas in organisms that have only one or two cistrons, resistance results from mutation of A2058 to G and from mutations in the other nucleotides near to the PTC that are critical for MLS binding (Vester 2001).

Erythromycin and related ribosomal inhibitors have two equivalent inhibitory effects on bacterial cells, inhibition of translation and inhibition of 50S ribosomal subunit assembly. Both activities of these drugs are responsible for their bactericidal effect in Gram-positive cells (Moazed and Noller 1987).

An understanding of the features of target sites is needed to understand the resistance mechanisms to antibacterial agents. A 3.1 Å X-ray crystal model of erythromycin with the 50S ribosomal subunit of *Deinococcus radiodurans* (Dr) provided important insights into the molecular basis of erythromycin binding to the ribosomes (Schlunzen et al. 2001). These crystal data indicate that macrolides attach in the peptide tunnel with the lactone ring about 25 Å from the subunit interface. The crystal structures reveal that the macrolides bind in a narrow part of the peptide exit tunnel at a site that lies between the peptidyl transferase center and the constriction in the tunnel near the proteins L4 and L22 and thereby occlude the lumen (Figure 4).

This, in turn, prevents the extension of nascent polypeptide chains (Weisblum 1985, Gregory and Dahlberg 1999).

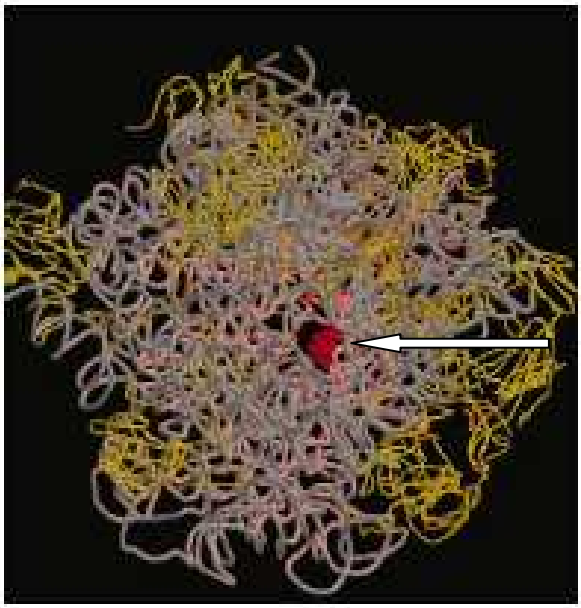

Figure 4 Top view of the *D. radiodurans* 50S subunit. Erythromycin (red) bound at the entrance of the tunnel is shown by white arrow. Yellow, ribosomal proteins; grey 23S rRNA; dark grey, 5S rRNA. Adapted from (Schlunzen et al. 2001).

Figure 5 depicts the detailed chemical interactions of erythromycin with ribosomes of *Deinococcus radiodurans* (Dr) as supported by the crystallographic studies. It shows that the 2'OH of the desosamine sugar forms hydrogen bonds at three positions: N6 and N1 of A 2041Dr (A2058 Ec) and N6 of A2042 Dr (A2059 Ec). The two hydrogen bonds between the 2'OH and the N1 and N6 of A2058 explain why this nucleotide is pivotal in macrolide binding, and also why dimethylation of N6 of A2058 is the most common mechanism of erythromycin resistance. The dimethylation of N6 of A2058 prevents hydrogen bonding of 2'OH group of the drug and also, more importantly, it adds bulky substituents onto the nucleotide causing steric hindrance for the binding of erythromycin. These studies implied that a

mutation of A2058 will disrupt the pattern of hydrogen bonding therefore impairing binding and rendering bacteria resistant.

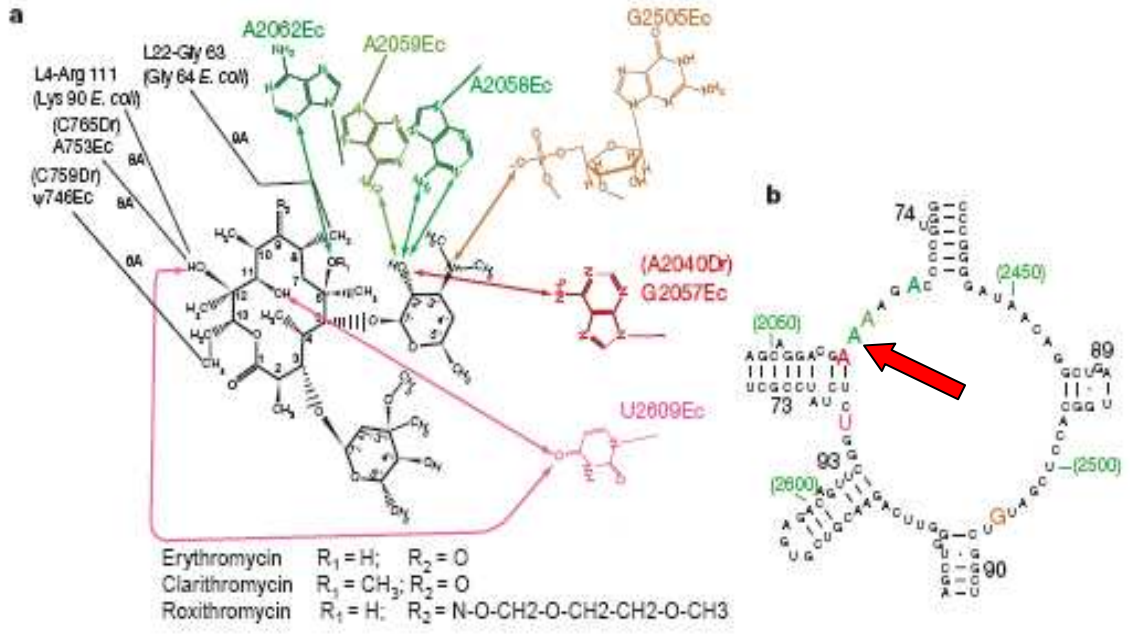

Figure 5 Interaction of Macrolides with Peptidyl Transferase Cavity: (a) Chemical structure diagram of the macrolides (erythromycin, clarithromycin and roxithromycin) showing the interactions of (colored arrows) of the reactive groups of the macrolides with the nucleotides of the peptidyl transferase cavity (colored). Colored arrows between the chemical moieties indicate that the two groups are less than 4.4 Å apart. (b) Secondary structure of peptidyl transferase ring of *D. radiodurans* showing the nucleotides involved in interaction with clindamycin (colored nucleotides). The colors in the secondary structure diagram match those of the chemical diagram. Nucleoties are numbered according to *E. coli* sequence. A2058 is indicated by an arrow (orange). Adapted from (Schlunzen et al. 2001)

Cladinose is suggested to be dispensable for binding and activity of erythromycin. The reactive groups of cladinose sugar are not involved in hydrogen-bond interactions with the 23S rRNA. This is confirmed by structure and activity

relationship (SAR) studies that showed the 4'OH is dispensable for macrolide binding (Mao and Putterman 1969).

Although ribosomal proteins can affect the binding and action of ribosome-targeted antibiotics, the primary target of antibiotics is the ribosomal RNA. One example where mutations in ribosomal proteins can lead to antibiotic resistance is in the loops of ribosomal proteins L4 and L22 that come close together in the wall of the peptide exit tunnel, very close to where MLS_B antibiotics bind (Chittum and Champney 1994). The mutations work in two different ways, either by preventing the drug binding (L4) or by neutralizing the effects of drug binding (L22) (Whittmann et al. 1973) . The ability of the ribosome to bind erythromycin is correlated with the width of the tunnel opening. In an L4 mutant, the tunnel becomes substantially narrower, which does not bind erythromycin, making the opening slightly smaller than the erythromycin A molecule. In contrast, the L22 mutant ribosome had an opening twice the size of the macrolide and hence is not inhibited by the latter (Gabashvilli and Gregory 2001). These observations further support a simple steric hindrance mechanism as the mechanism of action of this drug by binding inside the tunnel and blocking it, hence preventing the growth of the polypeptide chain.

As mentioned earlier, post-transcriptional modification of 23S rRNA is one of the well characterized mechanisms for erythromycin resistance. This is brought about by a class of enzymes, *erm* (erythromycin resistance methylase) group of methyltransferases (Gaynor and Mankin 2003). They specifically catalyze N-6 mono or dimethylation of a highly conserved adenine residue at 2058 (*E. coli* numbering equivalent to A2085 in *S. aureus*) in the domain V of 23S rRNA. These methyl groups encroach on the MLS_B binding site with in the peptide tunnel sterically hindering the binding of erythromycin.

This modification substantially reduces the binding of erythromycin to the exit tunnel that results in antibiotic resistance in *erm* carrying strains (Figure 6).

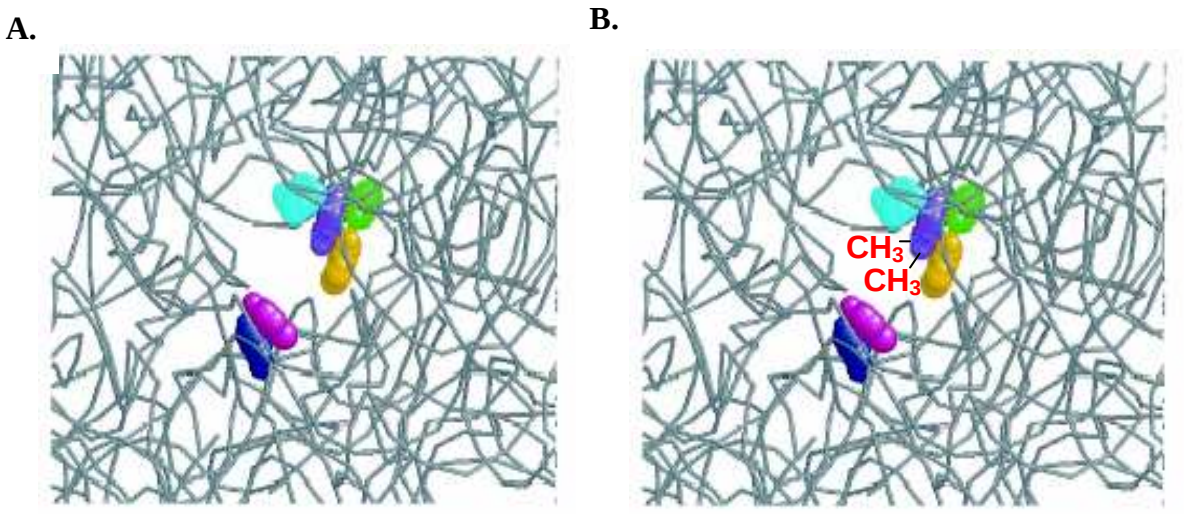

Figure 6 A. Close up view of the spatial arrangement of nucleotides involved in macrolide binding in the exit tunnel as seen from the peptidyl transferase side. rRNA is shown as grey backbone, while nucleotides involved in interaction with macrolide antibiotics are colored in a space-fill representation. Proteins were removed for clarity. Color representations: Green 2057, Yellow 2611, Blue 2058, Cyan 2059, Purple 2609, B. same as panel A with two methyl groups on A2058 (Orange). Adapted from (Garga-Ramos et al. 2002)

There are several rRNA *erm* methyltransferase isozymes conferring MLS_B phenotype. Although the corresponding *erm* genes present a substantial DNA sequence diversity, products of all genes methylate the N6 amine of A2058 in the 23S rRNA. All *erm* methyltransferases share a structurally homologous N-terminal catalytic domain that contains an S- adenosyl methionine (SAM) binding site that acts as the methyl group donor and a C-terminal RNA binding domain that holds the substrate. The methylases from erythromycin producers, *Streptomyces erytherus* (*erm* E) and *Arthrobacter* (*erm* F) are highly homologous (61%). The lowest levels of homology are between methylases from antibiotic producers (*erm* E, F) and non-producers *(erm* A, B, C and D) (18 to 24%) (Weisblum 1995).

Expression of *erm* methyltransferase can be induced by low concentrations of erythromycin. Erythromycin binds to ribosomes and the erythromycin-ribosome complex binds to the *erm* mRNA and changes its secondary structure. This facilitates expression of the *erm* gene in a process called translational attenuation (Grandi and Dubnau 1980, Vester et al. 1998). Inducibility is reversible and sensitivity to erythromycin is found after antibiotic removal.

Erm induction is well studied with the *erm* C gene expression. The inducible *erm* C cassette consists of two parts, the Erm gene whose expression is normally repressed due to sequestration of *erm* ribosome binding site in the secondary structure of mRNA and a constitutively expressed leader peptide cistron that precedes *erm*C (Dubnau 1985, Weisblum 1995) (Figure 7).

As shown in Fig 7A, in the uninduced ground state, segment 2 associates with segment 1 and segment 4 associates with segment 3. In this conformation, translation of *erm*C is initiated with a low efficiency because the first two codons of Erm C, AUG and AAU (fmet, Asn), as well as the ribosome binding site, are sequestered by the secondary structure. In this figure, Shine-Dalgarno sequences of the leader peptide (SD-1) and that of Erm cistron (SD-2) are also shown. Erythromycin induces the expression by favoring a translationally active conformation of *erm*C as shown in Figure 7B. When erythromycin binds to the ribosomes translating the 19 amino acid *erm*C leader peptide, the erythromycin-ribosome complex stalls around the 8^{th}-9^{th} codon of the leader peptide open reading frame. The stall of the ribosome triggers a conformational isomerization of the mRNA favoring the association of segments 2 and 3. This, in turn, opens up the *erm* ribosome binding site, and culminates in an increased efficiency of *erm*C translation. Removal of erythromycin or maximal

methylation of 23S rRNA results in an inactive conformation (Fig 7C). The conformational transition from 7B to 7A would also repress *erm*C, but energy would be required to dissociate stem 2:3. In contrast, the conformational transition from 7B to 7C would not require additional energy and hence is favored. Because the ribosome pauses while it is translating the leader peptide, this type of induction is called ”attenuation” and because the regulatory signal directly affects translation, this kind of mechanism of regulation is called ”translational attenuation”.

Erythromycin-Ribosome complex stalled on the leader peptide

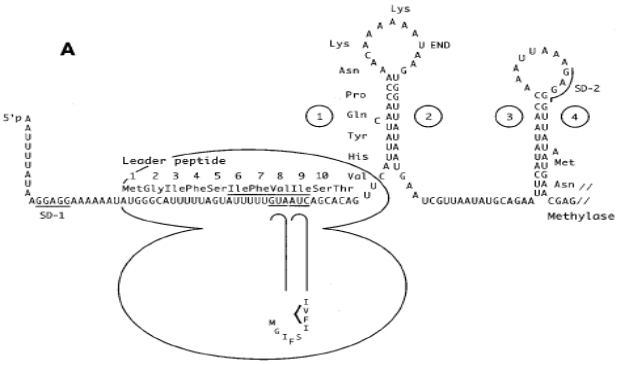

Fully induced state

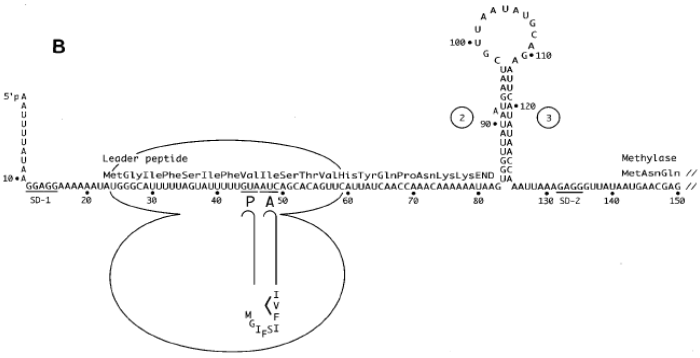

Repressed state

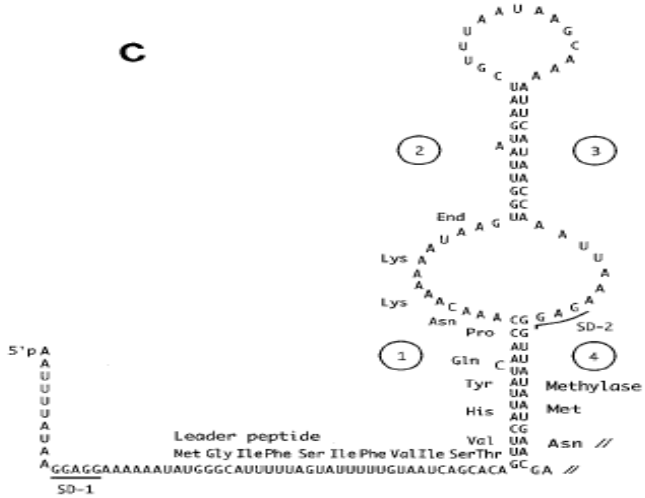

Figure 7 Conformational transitions of erm C leader sequence during induction
(A) Conformation of erm C mRNA early during induction by erythromycin. The four major segments of erm C attenuator are paired as segments 1:2 and segments 3:4 reflecting the temporal order of their synthesis. The ribosome is shown stalled during the addition of Ile-9 to the growing leader peptide. (B) Conformation of *erm*C leader mRNA during its fully induced state. (C) Inactive conformation of *erm*C mRNA. Adapted from (Weisblum 1995)

Because the stall on the leader ORF occurs only in the presence of the drug, the ribosome translating the leader peptide must bind the macrolide. On the other hand, for the translation of *erm*C cistron, ribosomes should be drug free. Thus the efficiency of *erm* induction depends critically on the macrolide concentration. Weisblum and colleagues have shown that induction of *erm*A expression occurred at 0.1 µM erythromycin and that resistant cells could be detected within 10 min of erythromycin addition (Weisblum et al 1985).

*Erm*E methyltransferase is one of the *erm* class enzymes that originates from the bacterium *Saccharopolyspora erythraea* that produces the macrolide antibiotic erythromycin (Skinner 1982). This gene must have evolved as a means of self defense. The recognition elements for the enzyme are contained within the domain V of 23S rRNA (Uchiyama 1985, Nielsen et al. 1999). It methylates protein free 23S rRNA in vitro, but 23S rRNA that is assembled into ribosomal subunits is no longer a substrate for the enzyme (Skinner 1983, Weisblum 1995). Thus, specific recognition of A2058 by the methyl transferase is directed by a motif in the 23S rRNA structure.

The sequence features of 23S rRNA needed for methylation are also known. The requirement for high enzyme fidelity in recognizing a single target A2058 amongst many other rRNA nucleotides suggests uniqueness and thus sequence complexity in this motif structure. Nucleotides close to A2058 in the primary and secondary structures of the rRNA have been implicated in the Erm methyltransferase interaction (Kovalic et al. 1995). In bacteria, the conservation of the nucleotides at positions 2055 and 2058-2061 is over 95%, but it is slightly lower for positions 2056 and 2057. However, the conservation of the secondary structure of this region is absolute, and the same irregular helix 73 structure is evident in all organisms. The ability of *erm*E

methyltransferase to modify 23S rRNA species from phylogenetically divergent bacterial species strongly suggests high level of conservation of secondary structure of the rRNA recognition motif.

Although 23S rRNA is the best studied in vitro substrate for *erm* methyltransferase, there is no free 23S rRNA existing in the cells. This is because as the ribosomal RNA is being synthesized it complexes with the ribosomal proteins to result in co-transcriptional assembly of 50S subunits. And, it was also found that fully assembled 50S subunits are not methylated by the enzyme (Champney 2003, Horinouchi 2006). A model for erythromycin inhibition predicts the accumulation of a stalled 50S precursor particle in erythromycin treated cells. Studies with *E. coli* have shown that a 50S precursor particle accumulates in erythromycin treated cells that co-sediments with the 30S subunits on the sucrose gradients (Figure 8).

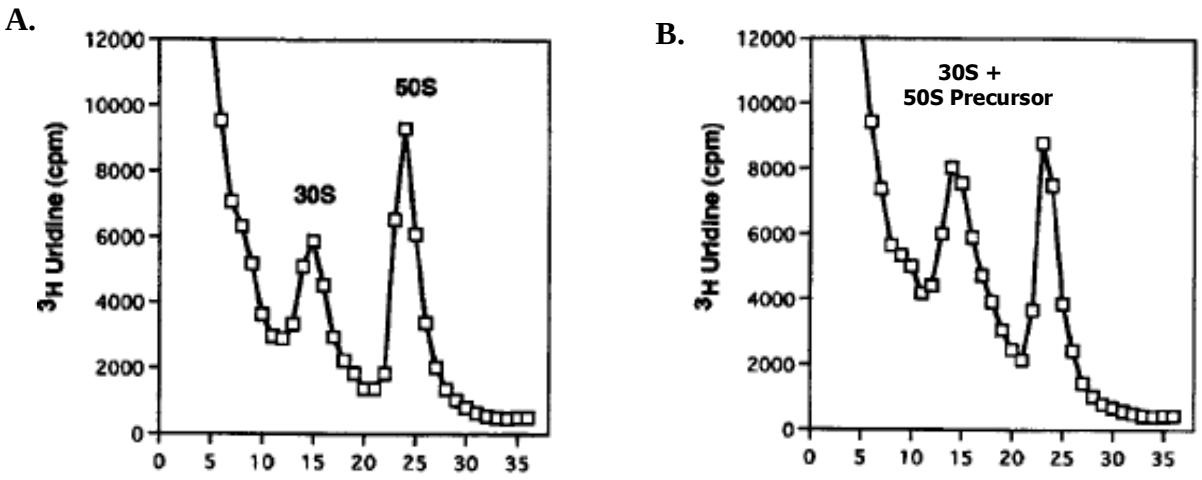

Figure 8 Sucrose gradient profiles of *S. aureus* RN 1786 cells grown without (A) and with (B) erythromycin. Cells were lysed with lysostaphin and layered on 5-20% sucrose gradients. Adapted from (Champney, Chittum, and Tober 2003)

.

Relief from inhibition and continued particle synthesis can occur by precursor methylation, which reduces erythromycin binding to 50S ribosomes. Previous studies from our lab used a partially purified *erm*C methyltransferase and an S1 nuclease protection assay to identify the protected methylated nucleotides. The probe was a 33-nucleotide DNA oligonucleotide complementary to *S. aureus* 23 rRNA sequences 2061-2094 that includes the single *erm*C modified nucleotide A2085. This oligonucleotide was hybridized to ^{3}H or ^{14}C methyl labeled rRNA samples, and after S1 nuclease treatment radioactivity in the protected fragment was measured. In cells grown in the absence of erythromycin, *erm*C methyltransferase modified A2085 was protected only in the rRNA isolated from the 50S region of the gradient, whereas in erythromycin treated cells, significantly, this protected rRNA was found in the 30S region of the gradient where the 50S precursor is predicted to accumulate (Figure 9).

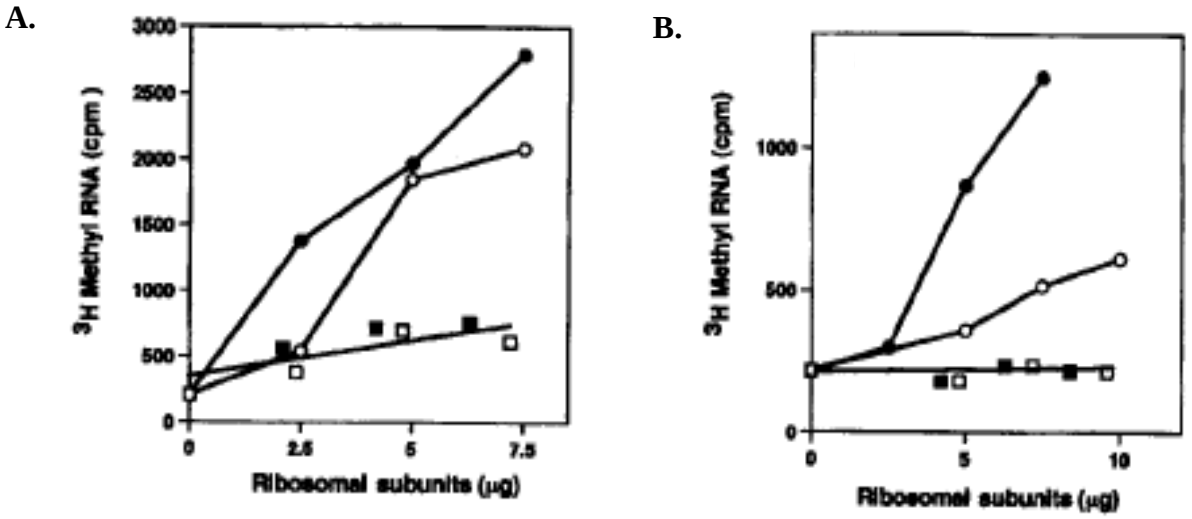

Figure 9 ErmC methyltransferase labeling of ribosomal subunits. (A) Methylation of 50S (□) and 30S(○) subunits from untreated cells. Methylation of 50S (■) and 30S(●) subunits from cells treated with erythromycin at 1µg/ml. (B) S1 nuclease protection assay on methylated sequences from 50S (□) and 30S (○) subunits from untreated cells. Nuclease protection assay on methylated sequences from 50S (■) and 30S (●) subunit gradient region from cells treated with erythromycin at 1 µg/ml. Adapted from (Champney, Chittum, and Tober 2003)

Based on these studies, a model has been proposed to explain the effects of erythromycin on ribosomes in wild-type and *erm* gene-containing cells (Figure 10) (Champney 2003). In cells lacking an *erm* gene, 50S subunit formation proceeds through the normal assembly sequence. In wild type organisms, erythromycin stalls 50S particle formation and the stalled subunit is degraded by the ribonucleases in the cell. In cells with an inducible *erm* gene erythromycin will also stall assembly of the nascent subunit. However, in this case the stalled precursor particle is a substrate for the induced *erm* methyltransferase enzyme. Methylation of 23S rRNA in the precursor particle relieves the assembly inhibition, permitting synthesis of methylated particles that are resistant to the inhibitory effects of the antibiotic. This assembly sequence explains why the mature 50S subunits are not methyltransferase substrates. Since cells do not contain protein free 23S rRNA and it was observed that mature 50S subunits are not substrates for the enzyme, the in vivo substrate for the enzyme is the 50S precursor particle that accumulates in the 30S region of the drug treated cells.

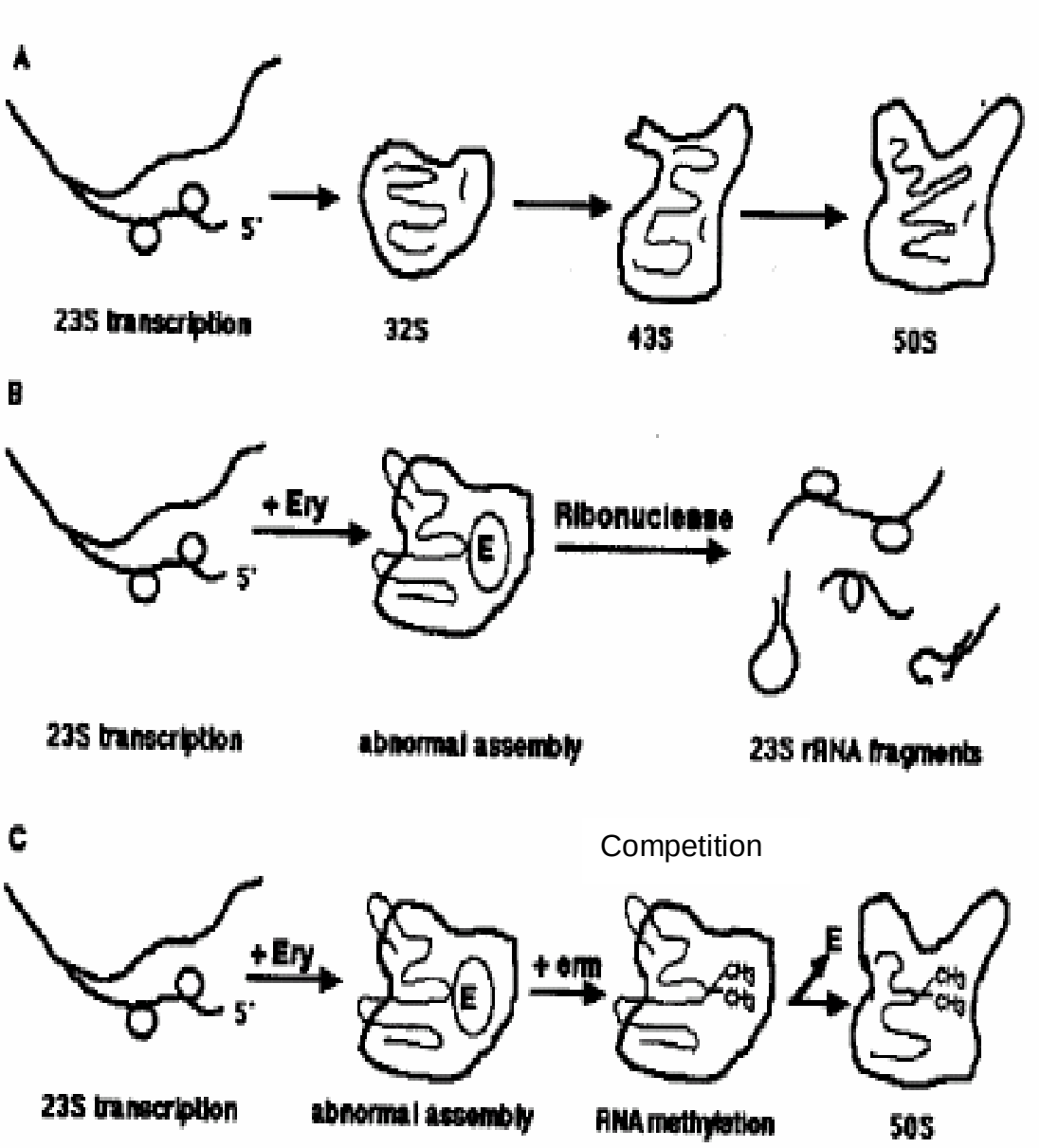

Figure 10 Model for the 50S subunit formation in *S. aureus* cells.
(A) Subunit formation in untreated control cells.
(B) Erythromycin-stimulated inhibition of 50S formation in antibiotic-sensitive cells.
(C) Reversal of erythromycin inhibition of subunit formation by *erm* methyltransferase in antibiotic-induced cells indicating competition between the two. (E=Erythromycin). Adapted from (Champney, Chittum, and Tober 2003)

The chief objectives of the current studies were to establish the 50S ribosomal precursor particle as the true in vivo substrate for the *erm*E methyltransferase enzyme and to characterize the ribosomal RNA and protein content of this precursor particle. Previous studies from our laboratory with *erm*C methyltransferase have shown that a 50S ribosomal subunit precursor particle that accumulates in the erythromycin induced cells acts as an important substrate for the enzyme (Champney et al. 2003). Observations from the S1 nuclease protection assay also corroborated a 50S precursor particle as a substrate for *erm* methyltransferase.

In the same studies when ribosomal subunits were used as enzyme substrates, it was found that 50S subunits were not substrates. Collectively, these results suggest that the 23S rRNA that is already assembled into 50S subunits is not methylated by the enzyme while the 23 rRNA in the 30S region of the erythromycin treated cells is a substrate. These observations further substantiate 50S precursor particle as the true in vivo substrate for the *erm* methyltransferase.

For the current studies, *Staphylococcus aureus* wild type strain RN 1786 that does not have an inducible *erm* gene was used (Koepsel 1985). It is hypothesized that the in vivo substrate for *erm*E methyltransferase is the 50S ribosomal precursor particle that sediments along with the 30S subunit region on the sucrose gradients. An additional hypothesis is that this precursor particle can bind erythromycin in vitro and that it consists of a subset of the 50S ribosomal proteins that are important for erythromycin binding and *erm*E methylation.

Another focal point of these studies was to examine the competition between erythromycin and *erm*E methyltransferase binding to the 50S precursor particle. In the cells with inducible *erm* gene, erythromycin induces the expression of *erm* methyltransferase that in turn methylates the stalled 50S assembly intermediate. This scenario suggests a competition between the enzyme and the drug for the same substrate, the 50S precursor particle. So, a further hypothesis was that, there would be a competition between MLS_B antibiotics and *erm*E methyltransferase for the 50S precursor particle in a concentration dependent manner.

An important factor here would be the stoichiometry of erythromycin binding to the ribosomes versus the *erm*E catalysis. As mentioned earlier, the predicted stoichiometry of erythromycin binding to the precursor particle is 1:1 where every single stalled precursor molecule would have one drug molecule bound. However, a single enzyme molecule can repeat the catalysis cycles to methylate more than one 50S precursor rendering them resistant. Hence, in the presence of *erm*, higher erythromycin concentrations would be needed to compete with the enzyme and to prevent the build up of methylated ribosomes. These predicted in vivo conditions indicate that in the presence of these two competing agents, the association constant (Kd) of the ribosome for either of them would determine whether a bacterial ribosome becomes resistant or not. This, in turn, would critically depend on their concentration. Understanding the competition phenomenon between the drug and the enzyme would be a significant step towards determining effective drug concentrations in organisms carrying resistance determinants.

One more vital goal of the current project was to characterize the ribosomal RNA and protein contents of the 50S precursor particle that accumulates in the presence of

erythromycin. Ribosomal RNA of the 50S precursor was identified by slot blot hybridization. As another part of these studies, the proportion of the 50S precursor particle in cells treated with increasing concentrations of erythromycin was also examined. Because it was previously shown that erythromycin binds to the ribosomes in 1:1 ratio, it would be logical to predict that with an increase in the drug concentration and a concomitant increase in 50S assembly stalling, the accumulation of the 50S precursor particle would also increase.

Protein characterization of the 50S precursor particle was performed by two-dimensional polyacrylamide gel electrophoresis and mass spectrometry. Previous studies from our laboratory with *E. coli* cells have shown that the 50S precursor can bind erythromycin in 1:1 ratio and that it contains 18 of the total 35 proteins of the 50S subunit (Usary and Champney 2001). 2D gel electrophoresis with the acidic first dimension and basic second dimension proved to be a successful technique for the otherwise hard to separate ribosomal proteins. But, unfortunately, unlike in *E. coli*, the ribosomal proteins of *S. aureus* were not well characterized. Hence to identify *S. aureus* ribosomal proteins on the 2D gels, molecular weights of the ribosomal proteins predicted from its genome sequence were used as an index (Holden et al. 2004).

Mass spectrometry is a powerful tool in protein analysis. Matrix-assisted laser desorption ionization (MALDI) (Karas et al 1987) time-of-flight (TOF) (Brown and Lennon 1995, Whittal and Li 1995), and electrospray (Fenn and Whitehouse 1989) technologies can be used to precisely detect changes in proteins and peptides. These techniques involve ionization of molecules into products that can be detected. The mass-to-charge ratio of gas phase ions can then be correlated with the molecular structure of the initial species. In MALDI, gas phase ions are generated by desorption

ionization of the molecule of interest from a layer of crystals formed from volatile matrix molecules. This technique has been used to detect all 56 ribosomal proteins of *E. coli* with posttranslational modifications and to detect alterations responsible for antibiotic resistance (Wilcox and Pearson 2001). In the current studies, MALDI-TOF mass spectrometry was used to identify the 50S proteins in the 50S precursor region of the erythromycin treated cells. The sensitivity of this method should ensure detection of all proteins.

Hydrophobic interaction chromatography (HIC) was used previously to purify bacterial ribosomes (Kirillov and Semenkov 1978, Ramakrishnan et al.1986, Saruyama 1986). One other aim of the current project was to evaluate HIC as a possible method to separate the 50S precursor from the 30S + 50S precursor mixture. Methylation of purified 50S precursor from the 30S, 50S precursor mixture would authenticate the former as the true in vivo substrate for *erm* methyltransferase. The principle of HIC is the difference in the hydrophobic interaction of the ribosomal subunits with the hydrophobic column material in low concentrations of Mg^{2+} ions. Because the 50S precursor particle is expected to have a different hydrophobicity than the 30S subunits, it should be possible to use HIC as a potential method for 50S precursor purification.

These studies will provide more information about the true nature of the substrate for the *erm*E methyltransferase, which is an important enzyme resulting in erythromycin resistance. Significantly, these studies will also focus on the competition between erythromycin and *erm*E methyltransferase for the 50S precursor particle that could potentially open up new targets for antibiotics. With the rapid emergence of

antibiotic resistant bacteria, it is essential to seek new antibiotic targets such as the 50S assembly intermediate.

CHAPTER 2

MATERIALS AND METHODS

Materials

Erythromycin, lincomycin, virginiamycin S, chloramphenicol, lysostaphin, DNAase I, RNA guard, Tris base, Tris-HCl, phenylmethylsulfonylfluoride (PMSF), Hepes, β-mercaptoethanol, Isopropyl Thio-Galactoside (IPTG), imidazole, and Octyl-Sepharose 6B were purchased from Sigma Chemical Corporation. Tryptic Soy Broth, tryptone, yeast extract, sucrose, urea, ammonium chloride, magnesium chloride, magnesium acetate, ammonium sulfate, glycine, glacial acetic acid, methanol, trichloro-acetic acid, phenol, chloroform, sodium lauryl sulfate (SDS), 2-propanol, formaldehyde, bovine serum albumin, sodium hydroxide, sodium chloride, potassium hydrogen phosphate (monobasic), potassium hydrogen phosphate (dibasic), sodium citrate, scintisafe gel scintillation fluid, Fuji-medical X-ray film, Kodak Film developer, and fixer were purchased from Fisher Scientific. Nytran SPC nylon transfer membranes for slot blot hybridizations were purchased from Scheicher & Schuell. Nitrocellulose membrane for Western blotting was purchased from Hoefer. SDS-PAGE low molecular range molecular weight standards and acrylamide were purchased from Biorad Inc. PCR primers were obtained from Life Technologies. The GF/A glass fiber filters and blotting paper were purchased from Whatman International. Millipore filters were purchased from Millipore Inc. ^{35}S-methionine (TRANS^{35}S-LABEL 1175 Ci/mmol) was purchased from MP Biomedical. ^{14}C Erythromycin (55 mCi/mmol) and Adenosyl-L-Methionine, S-(Methyl-^{3}H) (9.8 Ci/mmol) were purchased from PerkinElmer Lifesciences Inc, Boston, MA. Mouse anti-6His monoclonal antibody

(BD Biosciences) was a generous gift from Dr. Antonio Rusinol. Anti-Mouse IgG HRP conjugate was bought from Promega Corp, Madison.

Cricket Graph III software (Computer Associates) was used to construct graphs.

Curve fitting was also performed using Cricket Graph software. Curve fits were chosen according to best fit.

Labeling and Detection Kits:

1. Commassie Plus-Better Bradford Assay kit was purchased from Pierce Biotechnology.
2. Mirus Label-IT® biotin labeling kit was purchased from Fischer Scientific.
3. The North2South® chemiluminescent nucleic acid hybridization and detection kit was purchased from Pierce Chemical Corp. Washing, pre-hybridization solution, and background quencher were purchased from Molecular Research Center, Inc.
4. HIS-Select ^{TM} HC Nickel affinity gel was purchased from Sigma Chemical Co.

Bacterial Growth Media

1. Tryptic Soy Broth: 30 gm of Tryptic Soy Broth was dissolved in 1 L water and sterilized by autoclaving.
2. Luria Broth: 10 gm tryptone, 10 gm NaCl, and 5 gm of yeast extract were dissolved in water and pH was adjusted to 7.5 with 1.5 M NaOH and diluted up to 1 L.
3. A salts: 52.5 gm K_2HPO_4, 22.5 gm KH_2PO_4, 5.0 gm $(NH_4)_2$ SO_4, 2.5 gm Sodium citrate, 1 ml 20% $MgSO_4$ and made up to 1 L. (Miller 1972)
4. Staphylococcus Labeling Media (SLM): 1X A Salts supplemented with 10 gm/L NaCl, 0.2 gm/L Mg_2SO_4, 5 gm/L glucose, 2 gm/L desiccated beef extract (Difco), and 25 mg/L each of cysteine, tyrosine, and tryptophan. (Champney et al. 2003)

BUFFERS

1. SAS: 10 mM Tris-HCl, pH 8.0, 100 µM $MgCl_2$, 50 mM NH_4Cl
2. R Buffer: 10 mM Tris-HCl, pH 7.6,10 mM $MgCl_2$, 50 mM NH_4Cl, 2.8 mM β-mercaptoethanol
3. Wash Buffer: 25 mM Tris-HCl, pH 7.8, 60 mM KCl, 20 mM Magnesium acetate
4. Binding Buffer: 50 mM Tris-HCl, pH 7.8,80 mM KCl, 16 mM Magnesium acetate
5. Equilibration buffer: 50 mM sodium phosphate, pH 8.0, 0.3 M sodium chloride, 10 mM imidazole.
6. High salt wash buffer for *erm*E methyltransferase: 20 mM Tris-HCl, pH 8.0, 10 mM magnesium acetate, 6 mM β-mercaptoethanol, 1 M NH_4Cl, 10% glycerol
7. 2X Assay buffer : 100 mM Tris-HCl, pH 8.0, 8.0 mM $MgCl_2$, 80 mM KCl, 20 mM DTT, 12 mM NaCN
8. TE: 10 mM Tris-HCl, pH 7.8, 1 mM EDTA

Twelve Percent Polyacrylamide Gel Electrophoresis

1. Resolving gel solution: 1.8 ml 40% acrylamide-bisacrylmide, 1.5 ml of 1.5 M Tris –HCl, pH 8.8, 2.62 ml H_2O, 60 µl of 10% SDS, 6 µl TEMED and 60 µl 10% APS.
2. Stacking gel solution: 0.5 ml 40% acrylamide-bisacrylmide, 0.38 ml 1.0 M Tris-HCl pH 6.8, 2.1 ml H_2O, 30 µl 10% SDS, 3 µl of TEMED, 30 µl 10% APS.
3. 10 X SDS Running buffer: 30.3 gm Tris base, 144 gm glycine, 10 gm SDS in 1 L final volume
4. 2X SDS sample buffer: 125 mM Tris HCl, pH 6.8, 4% SDS, 20% Glycerol, 0.02% bromophenol blue

Two-Dimensional Gel Electrophoresis

2D sample buffer: 7.69 M Urea, 10 mM Bis-Tris, 0.6% glacial acetic acid, 144 mM β- mercaptoethanol.

1st Dimension:

1. Separating Gel Solution: 4% acrylamide, 0.132% bis-acrylamide, 8 M urea, 40 mM bis-tris, 0.45% acetic acid, pH 5.5.
2. Upper buffer: 2.5 ml 1 M Bis-Tris, 900 µl glacial acetic acid, make up to 250 ml with dH_2O, pH 3.8.
3. Lower buffer: 2.5 ml 1 M Bis-Tris, 100 µl glacial acetic acid, make up to 250 ml with dH_2O, pH 6.0. 1 ml of separating gel solution pH 5.5 was polymerized in the tube with 1 µl TEMED and 3 µl 10% ammonium per sulfate.
4. Dialysis buffer: 40 mM Bis-Tris, pH 6.0, 6.0 M urea, 1% SDS

SDS 2nd Dimension:

5. Upper buffer: 50 mM Bis-Tris MES, pH 6.5, 0.2% SDS
6. Lower buffer: 20 mM Bis-Tris acetic acid, pH 6.75
7. Resolving gel solution: 12.5 % Acrylamide, 0.25% Bis Acrylamide, 6 M urea, 0.1 M Bis-Tris acetic acid, pH 6.75. Resolving Gel solution was polymerized with 30 µl TEMED and 300 µl of 10% APS.
8. Stacking gel solution: 4% Acrylamide, 0.066% Bis Acrylamide, 6 M urea, 0.2% SDS, 0.04 M Bis-Tris acetic acid, pH 6.0. Stacking gel solution was polymerized with 20 µl of TEMED and 200 µl of 10% APS.
9. Sample buffer: 0.04 M Bis-Tris acetic acid pH 6.0, 8M urea, 1% SDS,

1% β-mercaptoethanol.

Slot-Blot Hybridization

1. Hybridization buffer: 50% formamide, 5X SSC, 0.1% Sarkosyl, 0.02% SDS, and 200 µg/ml BSA

Hydrophobic Interaction Chromatography

1. Buffer C: 10 mM magnesium acetate, 20 mM Hepes, pH 7.5.
2. Elution Buffer: Buffer C was mixed with $(NH_4)_2S0_4$ to give a final concentration of 0.1 M, 0.25 M, 0.5 M, 0.75 M, 1.0 M, 1.25 M or 1.5 M.

Western Blotting

1. Transfer Buffer: 25 mM Tris, 192 mM glycine, 20% Methanol, 0.025% SDS
2. TBST: 10 mM Tris-HCl, pH 8.0, 150 mM NaCl, 0.05% Tween-20

Bacterial Strains

1. *Staphylococcus aureus* strain RN 1786 was used for these current studies, provided by J. Sutcliffe of Pfizer (Koepsel et al. 1985).
2. *E.coli* DH1 cells transformed with plasmid perm 60, containing a cloned *erm*E gene encoding for *erm*E methyltransferase enzyme with a C-terminal His tag was a generous gift from Dr. S.R. Douthwaite (Vester et al. 1998).

Methods

Effect of Erythromycin on Cell Growth and Cell Viability

Erythromycin was dissolved in methanol at 10 mg/ml. RN 1786 cells were grown in TSB at 37^0C in the absence and presence of 1 µg/ml erythromycin. In some experiments, erythromycin was used at 0.1, 0.25, 0.5, 1.0 or 2.0 µg/ml concentrations. Cell growth was initiated by adding 1 ml of overnight culture to 20 ml TSB growth media. Cell growth was measured by following the increase in cell density in a Klett - Summerson colorimeter. The antibiotic was added at a Klett of 20 and cell growth was monitored over a period of two cell doublings. At this point 10 µl of the culture was added to 990 µl of 1x A salts, a serial dilution was performed to achieve a final dilution of 10^{-5} and 10 µl was plated on TSB agar plates (Jett and Hatter 1997). Plates were incubated at 37^0C for 24-48 hrs. The numbers of colonies formed were counted from control and drug treated cells to determine the effect of antibiotic on the total viable cell number.

Effect of Erythromycin on Protein Synthesis

Twenty ml cell cultures were grown as described above. After 2 cell doublings in the presence or absence of antibiotic, ^{35}S-methionine Trans label was added to the culture at a concentration of 1 µCi/ml. Three samples of 0.2 ml were removed at 5 minute intervals after the addition of the ^{35}S-methionine. Proteins were precipitated in 10% TCA and 0.2% BSA and were collected on Whatman GF/A glass fiber filters. The filters were washed with 10% TCA and 97% ethanol to ensure removal of free ^{35}S-methionine. Filters were air dried under a heat lamp and placed in vials with 3 ml Scintisafe Gel and radioactivity was measured by liquid scintillation counting.

Cell Lysis and Ribosomal Subunit Isolation

Cell lysis for ribosomal subunit and ribosomal RNA isolations were performed as described previously (Champney and Tober 1998). Cell pellets from 500 ml cultures were resuspended in 1 ml of SAS buffer, and 40 µg/ml lysostaphin, 0.1 M PMSF were added and lysis was carried out by incubating at 37^0C for 30 min. After incubation, cells were frozen for 5 min at -70^0C and thawed at room temperature. Freeze/thaw cycle was repeated 3 times. DNA in the samples was digested by adding 5 µg/ml DNAase I and incubating at room temperature for 10 min. Cell lysates were centrifuged at 4200 Xg for 10 min to separate the cell debris. Ribosomal subunits were isolated by centrifugation on 5-20% linear sucrose gradients. Gradients were made using a Buchler gradient maker and 18 ml each of 5% and 20% sucrose in SAS buffer. The clear lysate supernatant obtained above was layered on the prepared gradients and was placed in a SW27 swinging bucket rotor and centrifuged in a Beckman LE80K Ultracentrifuge at 42000 Xg for 18 hours. An ISCO Model UA-5 absorbance monitor was used to measure and record the absorbance at 254 nm of the gradients as they were pumped through. The 30S subunits were collected first followed by the 50S subunits. Subunits were precipitated by increasing the concentration of $MgCl_2$ to 1 mM and by adding 2 volumes of ice cold absolute ethanol. Ribosomal RNA was isolated from the subunits by phenol extraction. For this, an equal volume of Tris saturated phenol was added to the subunits, mixed by flipping the tube gently, kept on ice for 10 min and centrifuged in a microfuge at 10,000 rpm for 10 min. The aqueous supernatant was carefully recovered and equal volume of chloroform: isoamylalcohol (24:1) mixture was added, mixed by flipping gently, kept on ice

for 10 min and centrifuged at 10,000 rpm for 10 min. To the supernatant 2 volumes of ice cold ethanol was added and rRNA was precipitated overnight at -20^{0}C.

Purification of ermE Methyltransferase

An overnight culture of *E. coli* DH1 with perm60 was started by inoculating 5 ml of LB medium containing 100 µg/ml ampicillin with 0.5 ml glycerol stock an by adding. The next day, 500 ml of LB medium with 100 µg/ml ampicillin was inoculated with 1 ml overnight culture. At an optical density at 600 nm of 0.6, *erm*E expression was induced with 1 mM IPTG and cells were allowed to grow for another 3.5 hrs. Cells were harvested by centrifugation at 4200X g for 30 min followed by washing with 5 ml of R buffer and were frozen at -80^{0}C. Cell lysis was achieved by adding 100 µg/ml fresh lysozyme and 2.5 mM PMSF and incubating at 37^{0}C for 20 min until the solution turned turbid. The lysate was then subjected to 3 freeze thaw cycles, 5 U/ml of DNAase I was added and incubated at room temperature for 5-10 min until the turbidity cleared. Cell debris was cleared by centrifugation at 4200 X g for 10 min. The supernatant containing the ribosomes was pelleted down by spinning at 121000 X g for 3.5 hrs in Ti 50 rotor. *erm*E methyltransferase was obtained associated with the ribosomes. The enzyme was then washed from the ribosomes by suspending the pellet obtained in the previous step with high salt wash buffer containing 1 M NH_4Cl overnight. Crude extract of the enzyme was obtained by centrifugation at 121,000 X g for 3.5 hrs in Ti 50 rotor. Enzyme extract was then diluted to bring the salt concentration down 0.25 M.

Ni-affinity Chromatography

*erm*E methyltransferase with a C-terminal His- tag was further purified on HIS-Select ^{TM} HC Nickel affinity gel. The affinity gel was first washed with 1 to 2 volumes of deionized water to remove ethanol and then equilibrated with 5 volumes of equilibration buffer. Crude enzyme was mixed with the affinity gel and shaken on ice for 1-2 hrs. Unbound proteins were washed off the gel by equilibration buffer and the enzyme was eluted with elution buffer containing 250 mM imidazole. The eluate fractions were dialyzed into the R buffer with 10% glycerol to remove salts. Integrity of the enzyme was then assessed by Western blot using anti-6His Mouse monoclonal antibody.

Western Blotting

Integrity of *erm*E methyltransferase prepared above was determined by Western blotting using anti-6His mouse monoclonal antibody. Protein quantitation of the wash and elution fractions the Ni-affinity column and the crude enzyme fraction from the high salt wash of the ribosomes was done by Bradford reagent method in the test tube format (Commassie Plus-Better Bradford Assay, Pierce Biotechnology). For Bradford assay, a standard curve was obtained with BSA in the concentration range from 20 to 200 µg. Simultaneously, 100 µl of enzyme fractions were diluted to 1 ml with dH_2O and 1 ml of Commassie Plus reagent was added. Samples were allowed to stand at room temperature for 20 min and absorbance was measured at 595 nm. Concentration of protein was deduced form the BSA standard curve. Twenty µg of each sample was concentrated by precipitation with 5 volumes acetone overnight. Samples were centrifuged at 4200 X g for 30 min and the protein pellets were air dried. Dried samples were dissolved in 10 µl of water and an equal volume of 2X SDS sample buffer was

added. Samples were denatured by heating at 95^0C for 5 min and snap cooled on ice and briefly spun down. Samples were then subjected to 12% PAGE.

Twenty Percent SDS- Polyacrylamide Gel Electrophoresis

Twenty percent SDS-PAGE was carried out in the Biorad minigel apparatus. Electrophoresis was carried out in 1X SDS Running buffer at 50 V until the samples migrated into the resolving gel and then at 100 V until the bromophenol blue dye front migrated to the bottom of the gel.

At the end of the electrophoresis, the gel was pre equilibrated for 15 min in transfer buffer. A nitrocellulose membrane (pore size 0.45 µm, Hoefer) cut to the size of the gel, filter pads, and Whatman number 1 filter papers cut to the size of the filter pads were also soaked in the transfer buffer for 15 min. Transfer cassette was assembled according to the manufacturer's instructions of Biorad Mini Trans-Blot Cell. The gel sandwich was prepared with the grey side of the cassette down, followed on top by the pre-wetted filter pads and the filter paper. The pre-equilibrated gel was placed on the filter paper and the nitrocellulose membrane was placed on top of the gel. The cassette assembly was completed by placing the last filter paper and the filter pad. Any air bubbles trapped in the cassette were carefully removed by gently rolling a glass rod. Western transfer of proteins was carried by electro transfer in the Biorad Mini Trans-Blot Cell at 20 V overnight on a magnetic stirrer in the cold room at 4^0C. After the transfer, the nitrocellulose membrane was carefully removed from the cassette and further processed for the protein detection. All further operations were carried out at room temperature with gentle shaking.

1. Blocking: The membrane was blocked in TBST with 5% dry milk powder for 1 hr.
2. Primary antibody: Anti-6 His Mouse Monoclonal antibody (BD Biosciences) was diluted to 0.1 µg /ml with TBST with 5% milk and incubated with the membrane for 1 hr. Then the membrane was washed in TBST 3 times for 10 min each.
3. Secondary antibody: Anti Mouse IgG-HRP conjugate (Promega) was diluted 1 µl to 10 ml in TBST with 5% milk and added to the membrane, incubated for 1 hr.

Washes were carried out with TBST 6 times for 5 min each.

4. Detection: HRP substrate was made by mixing 1 ml peroxide and 1 ml luminal enhancer solutions (Pierce) just before use. They were added on the membrane and incubated for 5 min and decanted. Proteins were visualized by exposing the membrane to an X-ray film immediately. The exposure time was adjusted from 2 sec to 45 sec depending on the signal strength.

ermE Methyltransferase Activity Assay

*erm*E Methyltransferase activity assays were performed in a total volume of 100 µl containing, 20 pmols of the respective substrate (23S rRNA, 30S subunits, 50S precursor particle, 50S subunits, or 16S rRNA), 3 µCi of ^{3}H –S-adenosyl methionine, 30 pmols of the purified *erm*E methyltransferase enzyme, 50 µl of 2X assay buffer. After incubation at 37^{0}C for 20 min, reactions were stopped by adding 100 µl of TE buffer. ^{3}H Methylated RNA samples were extracted once with phenol and once with chloroform, then precipitated with 10% TCA. Samples were washed on GF/A glass fiber filters with 10% TCA and ethanol to wash off the unincorporated ^{3}H-S-adenosyl methionine. Filters were placed in vials with 3 ml Scintisafe Gel and ^{3}H methyl labeled RNA was counted by liquid scintillation counting.

MLS Inhibition of ermE Methylation

Erythromycin, lincosamide, and virginiamycin S were tested as inhibitors of *erm*E methylation. MLS drugs were diluted in 2X methylation assay buffer. To study inhibition by MLS drugs, *erm*E methyltransferase activity assay was carried out as described above but in the presence of a range of concentrations of MLS drugs from 0 to10 nmols. At the end of the incubation, reactions were stopped and samples were processed as described above for the methyltransferase assay.

^{14}C Erythromycin Binding Studies

^{14}C Erythromycin binding reactions were carried out in a final volume of 200 µl containing, 50 µl of binding buffer, 400 pmols of ^{14}C erythromycin, and 0, 20, 30, 40, and 80 pmols of one of the substrates (50S ribosomal subunits, 50S precursor particle, or 30S subunits). Samples were incubated at 37^{0}C for 20 min and the reactions were stopped by adding 2 ml binding buffer. Unbound ^{14}C erythromycin was washed off on Millipore membrane filters with 15 ml wash buffer and the bound ^{14}C erythromycin was counted by liquid scintillation counting.

ermE Methyltransferase and Erythromycin Competition Experiments

Competition experiments were carried out with fixed concentration of erythromycin and a range of concentrations of *erm*E methyltransferase. One set of assay reactions was set up with the concentration of erythromycin kept constant at 80 µM and 0, 0.32, 0.64, 0.96, 1.2, and 1.5 µM of *erm*E methyltransferase, 3 µCi of ^{3}H-S-adenosyl methionine, 50 µl of 2X assay buffer in a final volume of 125 µl. Another set of competition reactions was set up similarly but with ^{14}C erythromycin and unlabeled S-adenosyl methionine instead of

the unlabeled erythromycin and ^{3}H S-adenosyl methionine used in the first set. Reactions were incubated at 37^{0}C for 20 min and stopped by adding 100 µl of TE buffer at the end of the incubation period. In the first set of reactions, ^{3}H methyl RNA was extracted and counted as described for *erm*E methyltransferase assay. In the second set, bound ^{14}C erythromycin was quantified as described in ^{14}C erythromycin binding studies. Results were plotted on Cricket graph depicting either increase in ^{3}H methyl RNA formed or decrease in ^{14}C erythromycin bound as a function of *erm*E methyltransferase concentration.

Two-Dimensional Polyacryamide Gel Electrophoresis

Ribosomal proteins were isolated from twenty A260 units of 30S and 50S subunits of *Staphylococcus aureus* RN 1786 cells by acetic acid extraction and concentrated by precipitation with 5 volumes of acetone (Madzar et al.1979). After drying the sample, samples were suspended in 75 µl of 2D sample buffer pH 4.2 and gels were run as described.

First Dimension Gel Electrophoresis

The acidic first dimension gel electrophoresis was performed in glass tubes measuring 0.2 x 10 cm. Electrophoresis was carried out with cathode on top at 60V for 1 hr and then at 150V for 5 hrs.

Dialysis: First dimension gel was extruded from the glass tube and dialyzed for 1 hr in SDS- Dialysis buffer.

SDS- Second Dimension Gel Electrophoresis

Gels were cast in Hoefer SE500 Gel slab apparatus. An agarose plug was made with 3 µg of Low Molecular weight standards (95 Kd- 14 Kd, Biorad Inc). Electrophoresis was carried out with anode on top at 50 V for 1 hr and at 100 V for 5 hrs. The gel was stained with Commassie Brilliant Blue R 250 to detect protein spots.

MALDI-TOF Mass Spectrometry

Ribosomal protein samples were prepared from 30S and 50S subunits and 50S precursor region as described for the two-dimensional gel electrophoresis. After acetone precipitation, samples were dried in microfuge tubes and were analyzed by MALDI-TOF mass spectrometry at Columbia University Core Facility, New York. The Mass Spectrometer used was an Applied Biosystems Voyager DE Pro. Sample preparation and analysis was done as described by Wilcox et al. Briefly, samples were resuspended in 1% TFA to give 25 mg/ml. A saturated solution of sinapinic acid was prepared in a solution containing 30% acetonitrile and 0.1% TFA for the matrix solution. The sample for MALDI-TOF mass spectrometric analysis was then prepared by diluting 1.0 µl of protein solution to 10 µl with matrix solution and was spotted onto a flat, stainless steel target from PerSeptive Biosystems. MALDI-TOF data were collected on a PerSeptive Voyager Elite MALDI-TOF instrument with delayed extraction in positive-ion linear mode. Myoglobin was used to internally calibrate each spectrum.

A minimum of 150 µg of each sample was used for a single analysis. Resulting MALDI spectrum was analyzed and peaks corresponding with the molecular weights predicted from the *S. aureus* genome were identified. 50S proteins in the 30S + 50S

precursor mixture region were identified by comparing with control 30S and 50S proteins of *S. aureus*.

Slot-Blot Hybridization

A 101 bp biotinylated DNA oligonucleotide from *S. aureus* 23S ribosomal RNA sequence 2002-2103 was used as a probe that was complementary to a region of 23S rRNA that spans the *erm* methylation site of A2085. The probe was prepared by PCR amplification using the primers, F-GTAACGATTTGGGCACTGT and R-AAGCTCCACGGGTCT from Life Technologies. The PCR reaction mixture contained 45 µl of PCR Supermix High Fidelity reagent (Gibco BRL), 6 ng (1 µl) of *Staphylococcus aureus* RN 1786 total DNA, 1 µl (10 pmols) each of the forward and reverse primers, and 2 µl of sterile water. Samples were amplified for 35 cycles under the following conditions: denaturation at 94^0C for 30 s, annealing at 57^0C for 30 s, and extension at 72^0C for 30 s. The PCR products were purified by extraction with equal volume of phenol:chloroform and precipitated with 2 volumes of ethanol. The pellets were dried at 37^0C for 15 min and then resuspended in 30 µl of sterile water. The purified 50S precursor probe was labeled with biotin using Label-IT biotin labeling kit (Mirus Inc) following the manufacturer's instructions. Briefly, 50 µl of labeling reaction was set up with 5 µl each of 10X labeling buffer A, 5 µg of 101 bp DNA oligonucleotide probe and Label IT reagent and 35 µl of sterile water. The reaction mixture was incubated at 37^0C for 2 hrs. The biotin labeled probe was then purified on the microspin column provided with the kit. Just before use, the probe was denatured by 0.1 volume of denaturation buffer D1 (Mirus Inc.) by incubating at room temperature for 5 min followed by chilling

on ice for 5 min. The probe was then neutralized by 0.1 volume of neutralization buffer N1 (Mirus Inc.) and incubated at room temperature for another 5 min.

Ribosomal RNA was prepared from RN 1786 with phenol and chloroform extraction as described above. 23S rRNA (positive control) and 50S precursor region of the gradient were used in amounts 0.5, 1.0, 1.5, 2.0 and 5.0 µg of and the and 2 µg of 16S rRNA (negative control) were spotted on a nylon membrane (Nytran, Schleicher & Schuell) using the slot blot apparatus. RNA was cross linked to the membrane in a UV Crosslinker oven (FisherBiotech). The membrane was pre-hybridized at 42^0C for 30 min in 15 ml of 1X Prehybridization solution. The membrane was hybridized at 42^0C overnight in 7 ml of hybridization buffer with 1X background quencher (MRC Inc.) and 4 pmols of denatured 50S precursor probe prepared as described above. Following hybridization, the membrane was washed and the biotinylated probe was detected using the North2South chemiluminescent hybridization kit (Pierce Chemical Co.) according to the manufacturer's instructions.

A standard curve was obtained for the 23S rRNA based on the signal intensity of each spot quantified by AlfaImager^{TM} 2200 Documentation & Analysis System (Alfa Innotech Corp. San Leandro, California). The images on the slot blot containing the 50S precursor samples were also scanned to obtain Integration Density Values (IDV) that are direct measures of the signal intensity. From these IDVs, the amount of 23S rRNA present in 2 µg of each 30S+ 50S precursor mixture sample was calculated from the 23S standard curve. This yielded the percentage of 23S rRNA in each sample, which is a direct measure of percentage of 50S precursor particle in the 30S region of erythromycin treated cells.

Hydrophobic Interaction Chromatography

The 50S precursor particle was separated from the 30S + 50S precursor mixture by hydrophobic interaction chromatography. Octyl-Sepharose 6B was used as the hydrophobic matrix and was poured in a 15 x 1 cm column (Pharmacia Fine Chemicals, Uppsala, Sweden). The column was equilibrated with buffer C with a stepwise increase in ammonium sulfate concentration from 0.1 M to 1.5 M. Equilibration was carried out until the pH of buffer eluting from the column was the same as that of the equilibration buffer applied on top of the column. ^{35}S-Methionine labeled ribosomal subunits were applied on the column and eluted with a stepwise reverse gradient of ammonium sulfate from 1.5 M to 0.1 M. Fractions were collected at each salt concentration (1.5 M, 1.25 M, 1.0 M, 0.75 M, 0.5 M, 0.25 M, and 0.1 M). The ^{35}S-Methionine radioactivity in the eluted fractions was measured by liquid scintillation counting.

Methylation of HIC column Fractions

Fractions collected at each ammonium sulfate concentration were pooled and precipitated with 2 volumes of ice cold ethanol at -20^{0}C overnight followed by centrifugation at 4200 X g for 20 min. Salts were removed by passing through Sephadex G-25. The rRNA content was quantitated by measuring A260. Methylation assays were carried out as described above in *erm*E methyltransferase assay using 20 pmols of rRNA from each fraction as the substrate.

CHAPTER 3

RESULTS

Effect of Erythromycin on Growth Rate, Cell Viability, and Protein Synthesis of *Staphylococcus aureus*

Erythromycin is a macrolide antibiotic that has been widely used as an antimicrobial agent against a variety of bacteria, especially Gram-positive cocci (Omura 1984). Numerous studies from our lab have revealed that this antibiotic inhibits 50S subunit assembly as effectively as it does the protein synthesis (Champney 2003). Previous studies indicated that 0.5 µg/ml erythromycin impaired vital cell activities like the growth rate, cell viability and protein synthesis significantly in *S. aureus* RN 1786 (Champney and Tober 1998). The current set of experiments is designed to test if increasing concentrations of erythromycin will increasingly inhibit growth rate, cell viability, and protein synthesis.

For these experiments, *S. aureus* strain RN 1786 was grown in TSB with different concentrations of erythromycin ranging from 0.1 to 2.0 µg/ml. Growth curves are shown in Figure11. The results indicate that growth was inhibited in the presence of the antibiotic. Also, at higher concentrations of erythromycin, growth rate inhibition was more pronounced as evident from the increased cell doubling time. Figure 12 A shows the decline in growth rate as the percent of the control growth rate as the concentration of erythromycin increases.

Cells grown in erythromycin were diluted and plated on TSB agar plates and colonies were counted to see the effect of erythromycin on TVC. Results in Figure 12 B show that as the concentration of erythromycin increases there is a decrease in TVC.

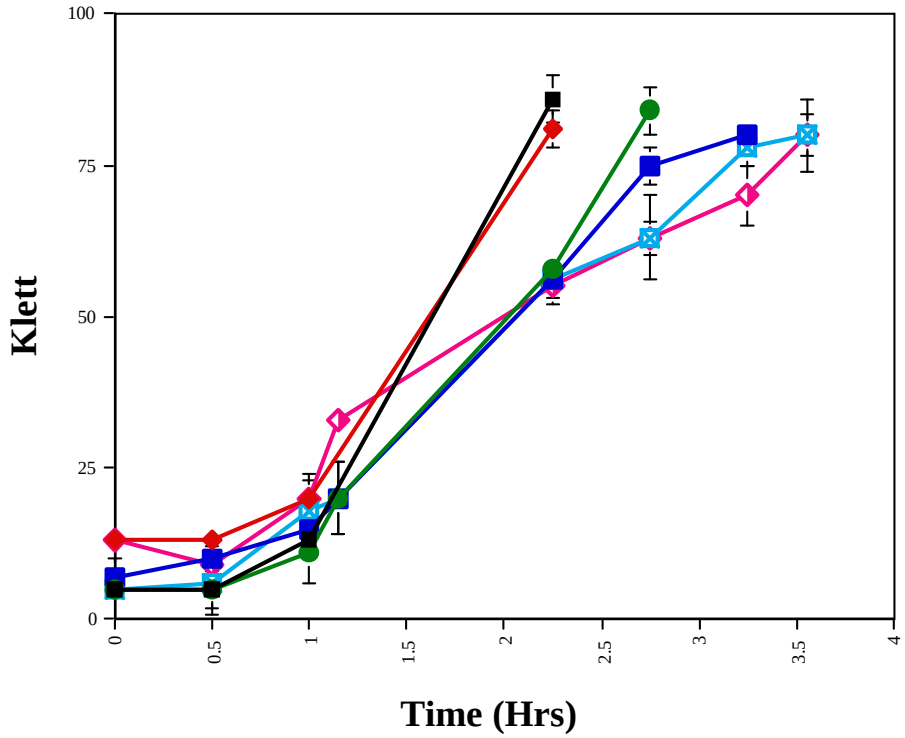

Figure11 Inhibition of cell growth by erythromycin in RN 1786: Cells were grown with erythromycin at 0 µg/ml (■), 0.1 µg/ml (♦), 0.25 µg/ml (◕), 0.5 µg/ml (■), 1.0 µg/ml (▣), and 2.0 µg/ml (◪). Results are means of three experiments. Bars indicate SEM.

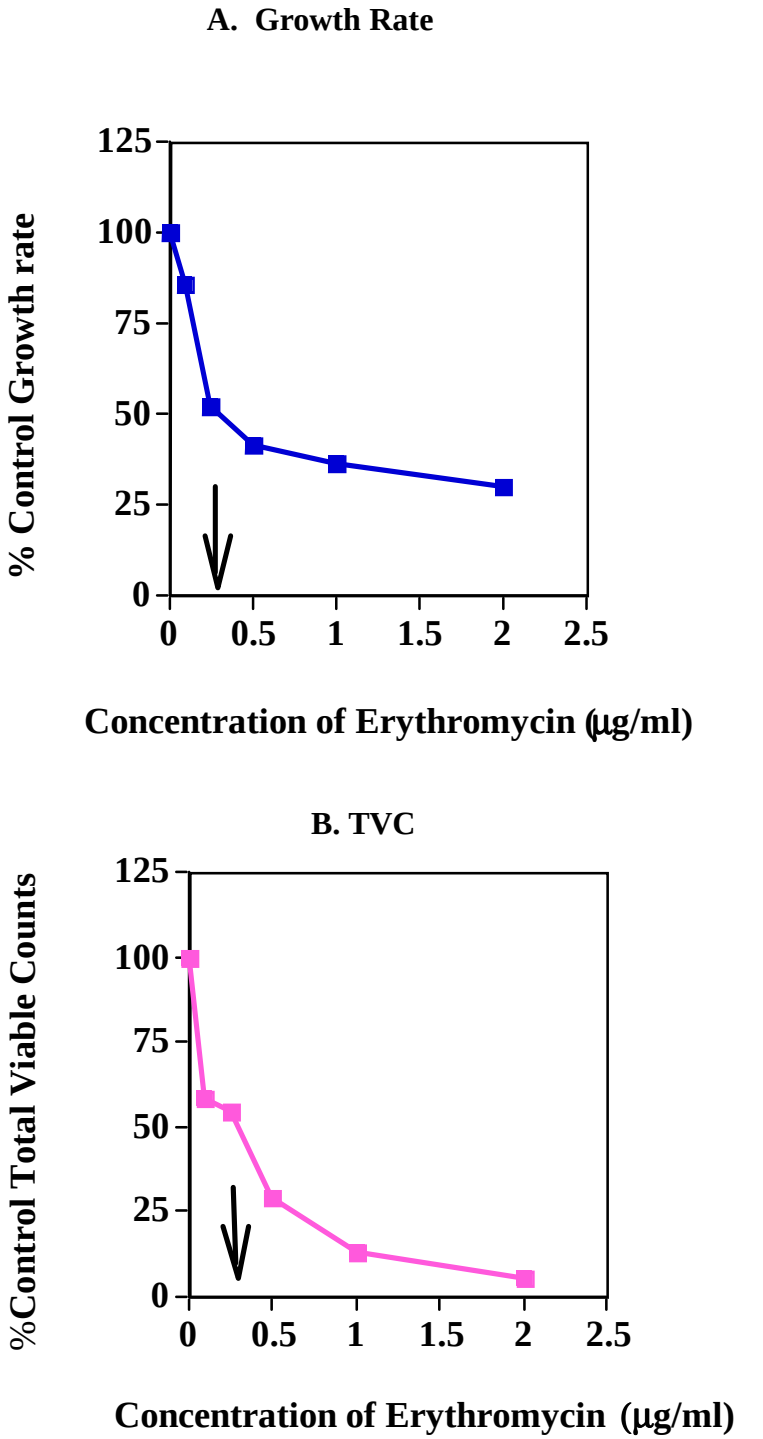

Figure 12 Percent Inhibition of Growth rate and Total Viable Counts in RN 1786 with Erythromycin**:** Cells were grown with a range of concentrations of erythromycin as described in Fig. 11 and the results were plotted either as (A) percent control growth

rate or (B) percent control TVC. Arrows indicate respective IC_{50} values. Results plotted are the means of three experiments. Bars indicate SEM.

The inhibition of protein synthesis by erythromycin was studied in RN 1786. Figure 13 A depicts the increased inhibition of protein synthesis in RN 1786, which declined with the concentration of erythromycin. Figure 13 B illustrates the decline in protein synthesis as percent of control protein synthesis with the arrow indicating the IC_{50} value.

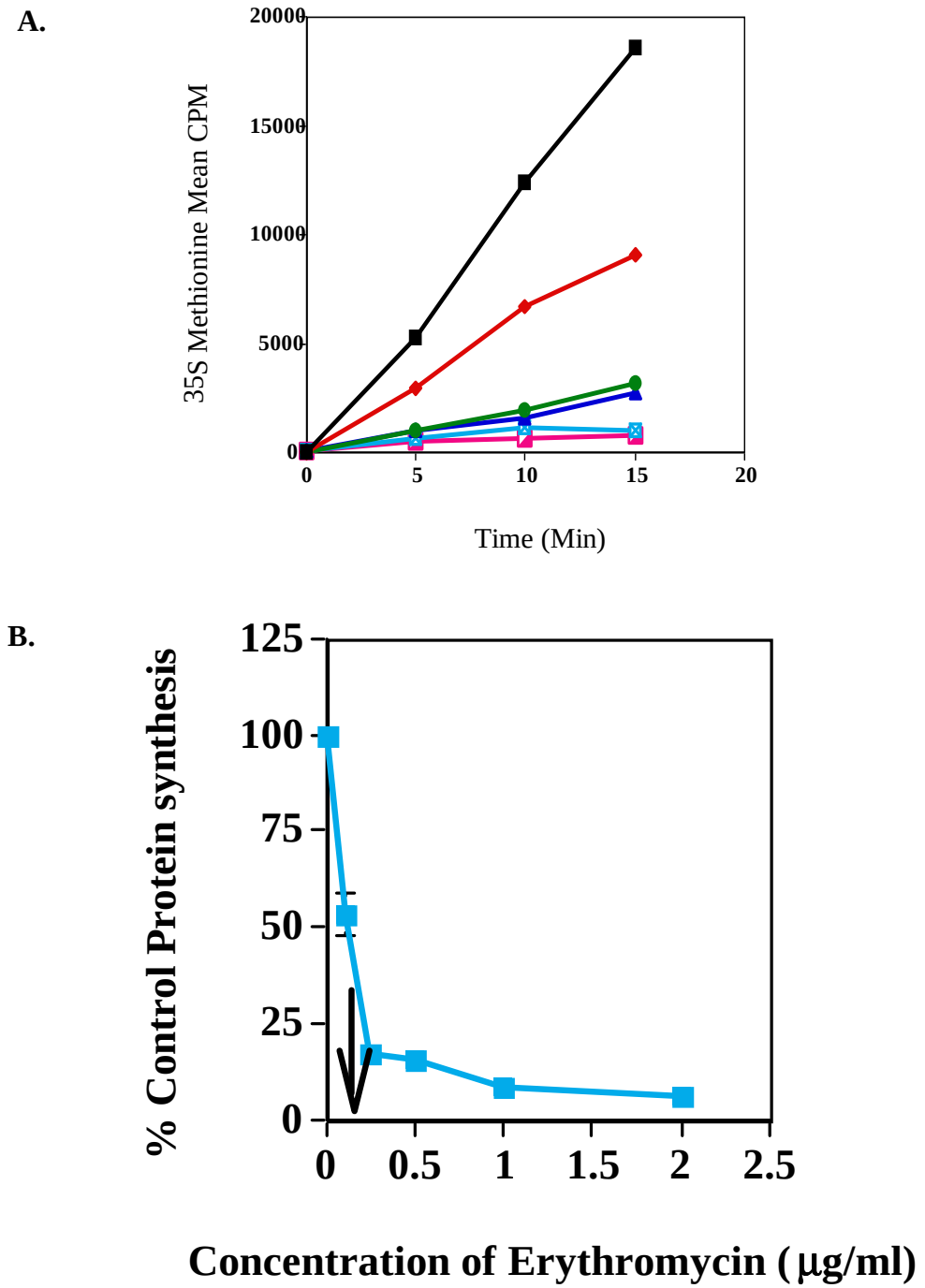

Figure 13 Inhibition of protein synthesis in RN 1786 by erythromycin. (A) Inhibition of ^{35}S-methionine incorporation in RN 1786 cells treated with erythromycin at 0 µg/ml (■), 0.1 µg/ml (♦), 0.25 µg/ml (◓), 0.5 µg/ml (▲), 1.0 µg/ml (⊠), and 2.0 µg/ml (◪). (B) Results from A were plotted as percent control protein synthesis. Arrow indicates IC_{50}. Results are the means of three experiments. Bars indicate SEM.

IC_{50} was measured based on the concentration of erythromycin required for 50% inhibition of growth rate, total viable cell counts, and protein synthesis. Results are given in Table1.

Table 1IC_{50}Values (µg/ml) for Erythromycin Inhibition

Growth rate	**Viable Cell Count**	**Protein Synthesis**
0.31 ± 0.08	0.28 ± 0.06	0.21 ± 0.03

Arrows in Figures 12A and 12B and 13B indicate respective IC_{50} values. Results are the means of two experiments. ± indicates SEM.

Characterization of the 50S Subunit Precursor Particle

Multiple studies from our lab have shown that a 50S precursor particle accumulates in erythromycin treated cells and that it sediments along with the 30S subunits on the sucrose gradients of the lysates from the drug treated cells. Previously, studies with *E. coli* from our lab indicated that this 50S precursor particle contains 23S rRNA and 18 of the large subunit ribosomal proteins (Usary and Champney 2001). Motivated by these observations, current experiments are designed to examine whether the same pattern could be observed in *S. aureus*. It is hypothesized that the 50S precursor particle that accumulates in erythromycin treated cells contains 23S rRNA whose concentration in this precursor region will increase as the concentration of erythromycin increases. To verify this hypothesis slot-blot hybridizations were performed. An additional hypothesis to be tested is that the precursor region will contain

a subset of *S. aureus* 50S ribosomal proteins. To test this hypothesis, two-dimensional electrophoresis was used to analyze *S. aureus* ribosomal proteins and the precursor protein content was studied by MALDI-TOF mass spectrometry. For all the studies the 50S precursor particle used was a mixture of 50S precursor + 30S subunits. In order to separate the 50S precursor from this mixture, hydrophobic interaction chromatography was employed.

Slot -Blot Hybridization for 23S rRNA Analysis

To quantify the amount of 23S rRNA and hence that of 50S precursor particle in the 30S region of the drug treated cells, slot blot hybridization procedure was used. Initially a range of concentrations of 23S rRNA from 0.5 – 5 µg were slot blotted on the nylon membrane and their hybridization signal intensities were quantified by densitometric analysis. A biotinylated 101 base length DNA oligonucloetide was used as a probe that spans *S. aureus* 23S sequences from nucleotides 2002-2103. From this a standard curve was obtained for 23S rRNA which was shown in Figure 14. This standard curve was used to quantify 50S precursor particle amounts in erythromycin treated cells.

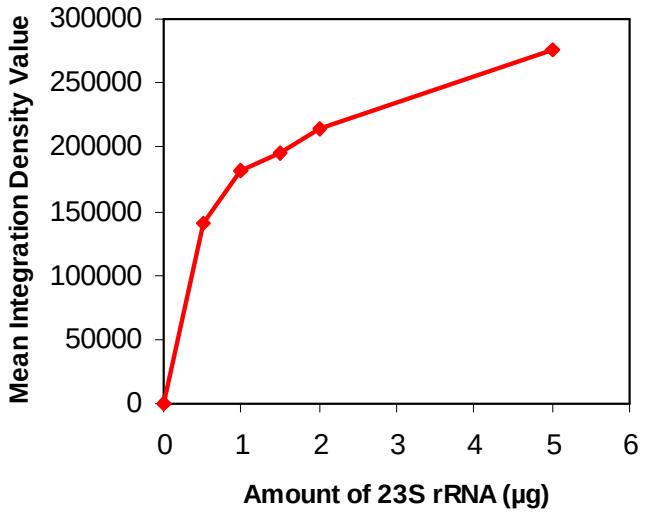

Figure 14 23S rRNA standard curve by slot blot hybridization: 23S rRNA was isolated from RN 1786 cells and slot blotted onto Nytran membrane at concentrations 0 µg, 0.5 µg, 1.0 µg, 1.5 µg, 2.0 µg, and 5.0 µg. Hybridization was performed with a biotin labeled 23S rRNA specific probe and the images were scanned by AlfaEase™ software to obtain IDV values. Results shown are the means of two experiments.

Quantitation of the 50S Subunit Precursor Particle

Slot Blot hybridization with the 101 bp biotinylated DNA probe for the 23S rRNA was performed to characterize and quantify the 50S precursor particle in the 30S+50S precursor particle mixture of RN 1786 cells. Figure 15A shows the slot-blot hybridization results for positive (23S rRNA) and negative (16S rRNA) controls along with those for the 50S precursor particle. 23S rRNA showed a strong hybridization signal whereas there was no hybridization signal with the 16S rRNA indicating the high specificity of the probe for the 23S rRNA. Figure 15B shows the results obtained for 50S precursor particle from cells treated with different concentrations of erythromycin. Ribosomal RNA obtained from the 30S+50S precursor region showed increasing hybridization signal with increasing erythromycin concentration indicating an increasing accumulation of the 50S precursor particle. 23S rRNA showed a strong hybridization signal.

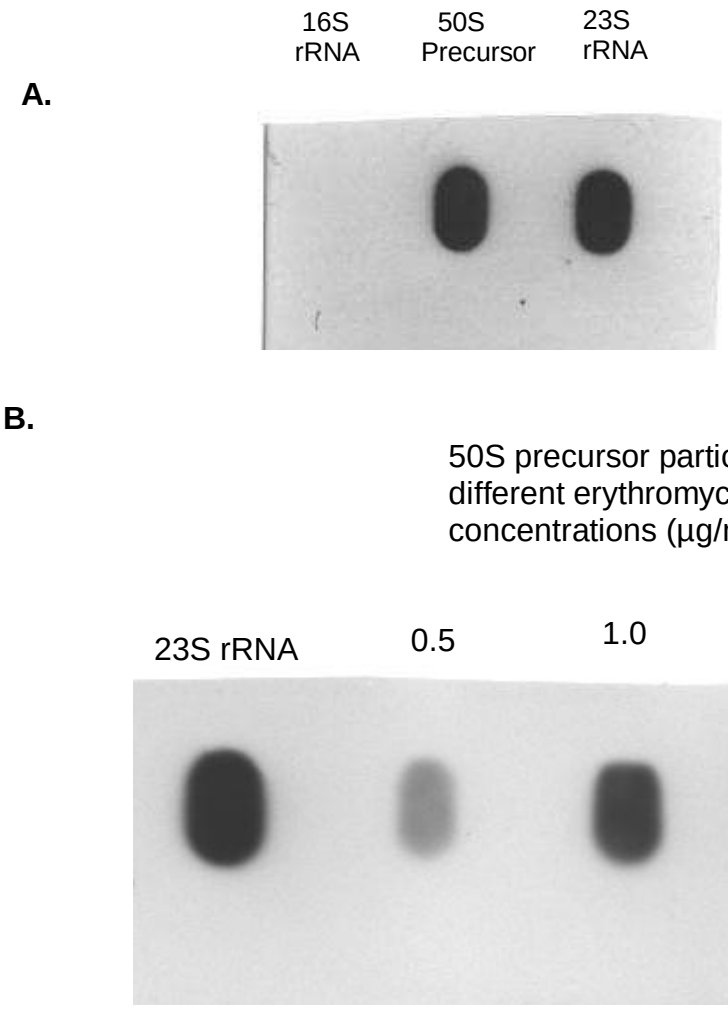

Figure 15 Characterization and Quantitation of 50S precursor particle by slot blot hybridization: A. Ribosomal RNA was isolated from 30S subunits from control cells (16S rRNA), 30S subunit+50S precursor region of the erythromycin treated cells (50S precursor), and from the 50S subunits of the control cells (23S rRNA). 2.0 µg of each sample was spotted and hybridized as described in B.
B. Ribosomal RNA from the 30S region with the 50S precursor particles of RN 1786 cells treated with 0.5 µg/ml,1.0 µg/ml, and 2.0 µg/ml of erythromycin was isolated. 2.0 µg of rRNA from each sample was blotted onto Nytran membrane along with 2.0 µg of 23S rRNA as positive control and hybridized with a biotinylated 23S rRNA specific probe. Images were scanned on AlfaEase™ and the amount of 23S rRNA in each sample was quantified from the 23S rRNA standard curve as described in Methods.

From the IDV values (Table 2) obtained for images in Figure 15B, the percentage of 23S rRNA and hence the 50S precursor present in each sample of 30S + 50S precursor mixture was calculated as described in Methods. These results were tabulated in Table 3.

Table 2 IDV values for the images in Figure 15B

Concentration of Erythromycin (µg/ml)	Normalized Mean IDV
0.5	83640 ± 198
1.0	111366 ± 229
2.0	157420 ± 272

Images were scanned by AlfaEase™software and from the IDV values obtained, percentage of 50S precursor in each sample was calculated using the 23S rRNA standard curve (Figure 14). Results are the means of three experiments. ± indicates SEM.

Table 3 Quantitation of 50S precursor particle

Concentration of Erythromycin (µg/ml)	% Protein synthesis	% 50S precursor/ Total RNA
0.5	15.8 ± 1.01	15 ± 2.42
1.0	8.8 ± 1.55	22 ± 3.16
2.0	6.6 ± 1.41	57 ± 4.71

Ribosomal RNA was isolated from RN 1786 cells treated with increasing concentrations of erythromycin. The amount of 23S rRNA in the 30S+50S precursor region was quantified by slotblot hybridization followed by scanning with AlfaEase™software. Results shown are the means of three experiments. ± indicates SEM.

These results indicate that there was an increased accumulation of 50S precursor particle as the concentration of erythromycin was increased. At 2.0 µg/ml erythromycin, 57% of the rRNA from the 30S+50S precursor mixture was 23S rRNA indicating there could be 43% 16S rRNA. The decreases in protein synthesis rates and the viable cell counts along with the simultaneous increases in the 50S precursor particle accumulation as a function of erythromycin concentration are shown in Figure 16.

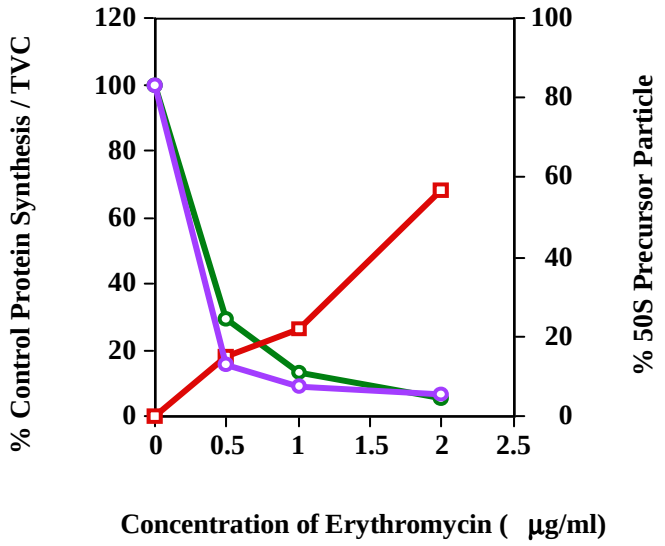

Figure 16 Comparison of effect of erythromycin on different cellular activities in RN 1786: protein synthesis (O), viable cell count (O), and percentage of 50S precursor particle (□). Results shown are the means of three experiments. Bars indicate SEM.

Two- dimensional Gel Electrophoresis of S. aureus Ribosomal Proteins

Two dimensional gel electrophoresis was performed to analyze the ribosomal proteins of *S. aureus* that has not been studied previously. Both 30S and 50S ribosomal subunit proteins of *S. aureus* were analyzed to establish their electrophoretic mobility patterns. SDS gel electrophoresis with molecular weight standards was carried out in the second dimension for molecular weight estimates of ribosomal proteins. Figures 17 and 18 show the gel patterns for 50S and 30S subunits from control RN 1786 cells respectively. Thirty five protein spots were identified in the 50S gel and twenty-one spots in the 30S gel are seen.

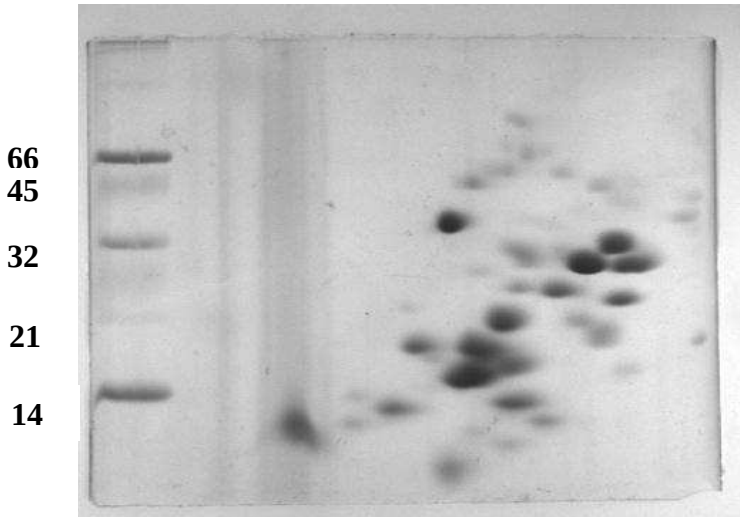

Figure 17 SDS-2D gel electrophoresis of 50S ribosomal subunits of *S. aureus* RN 1786. Molecular weight standards are marked on the left.

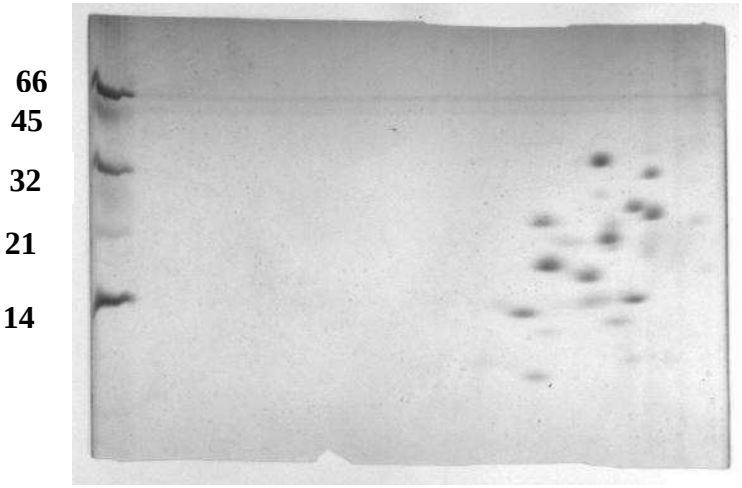

Figure 18 SDS 2D gel electrophoresis of 30S subunits of *S. aureus* RN 1786. Molecular weight standards are indicated on the left.

Molecular weight standards were electrophoresed simultaneously. Individual proteins were identified by correlating their corresponding molecular weights on the gel to those predicted from the genome analysis (Holden et al. 2004). Characteristics of *Staphylococcus aureus* ribosomal proteins as predicted by genome analysis are given in Tables 4 (50S) and 5 (30S).

Table 4 Characteristics of *S. aureus* 50S ribosomal proteins predicted by the genome analysis (Holden et al 2004)

50S Protein	Gene ID	Sequence Location	Predicted No. of Amino acids	Predicted Post. Translational Modifications	Predicted Mol wt (KDa)
L1	2860898	rplA/SAR0543	229		24.4
L2	2860899	rplB/SAR2332	277		30
L3	2860900	rplC/SAR2335	220	Met Gln 150	23.5
L4	2860901	rplD/SAR2334	207		22.3
L5	2860902	rplE/SAR2323	179		20.1
L6	2860903	rplF/SRA2320	178		19.6
L7/L12	9860907	rplL/SAR0545		Ac Ser 1, Met Lys 81	12.6
L8			122		
L9	2860904	rpsF/SAR0362	148		16.3
L10	2860905	rplJ/SAR0544	166		17.5
L11				Tri Met Ala 1, Tri Met Lys 3, Tri Met Lys 39	14.7
L12	2860906	rplK/SAR0542	140		
L13	2860908	rplM/SAR2301	145		16.2
L14	2860909	rplN/SAR2325	122		13
L15	2860910	rplO/SRA2316	146		15.4
L16	2860911	rplP/SAR2328	144	Met Met 1, Arg der 81	16.1
L17	2860912	rplQ/SAR2308	122		13.6
L18	2860913	rplR/SRA2319	119		12.9
L19	2860914	rplS/ SAR1217	116		13.2
L20	2860915	rplT/SAR1758	118		13.5
L21	2860916	rplU/SAR1727	102		11.2
L22	2860917	rplV/SAR2330	117		12.7
L23	2860918	rplW/SAR2333	91		10.4
L24	2860919	rplX/SAR2324	105		11.4
L25	2860920	rplY/SAR0502	217		23.7
L26					
L27	2860921	rpmA/SAR1725	94		10.1
L28	2860922	rpmB/SAR1200	62		6.8
L29	2860923	rpmC/SAR2327	69		7.9
L30	2860924	rpmD/SRA2317	59		6.4
L31	2860925	rpmE/SRA2208	84		9.5
L32	2860161	rpmF/SAR1101	57		6.3
L33 type1	2860162	rpmG1/SAR1628	49	Met Ala 1	5.7
L33 type 2	2860163	rpmG2/SAR1345	49		5.8
L33 type 3	2860164	rpmG3/SAR0538	47		5.7
L34	2860165	rpmH/SAR2800	45		5.3
L35	2860166	rpmI/SAR1759	66		7.5
L36	2860167	rpmJ/SAR2312	37		4.1

Table 5 Characteristics of *S. aureus* 30S ribosomal proteins predicted by genome analysis (Holden et al. 2004)

Protein	Gene ID	Sequence Location	Predicted No. of Amino acids	Predicted Post. Translational Modifications	Predicted Mol wt (KDa)
S1	2860032	SAR1485	391		43.1
S2	2860173	rpsB/SAR1232	255		28.9
S3	2860174	rpsC/SAR2329	217		23.9
S4	2860175	rpsD/SAR1797	200		22.8
S5	2860176	rpsE/SRA2318	166	1 Ac Ala	17.6
S6	2860177	rpsF/SAR0362	98		11.4
S7	2860178	rpsG/SAR0551	156		17.6
S8	2860179	rpsH/SRA2321	132		14.7
S9	2860180	rpsI/SRA2300			14.4
S10	2861446	rpsJ/SAR2336	102		11.4
S11	2661447	rpsK/SAR2310	129	1 Met Ala	13.7
S12	2861448	rpsL/sar0550	137	88 Asp derivative	15.1
S13	2861449	rpsM/SAR2311	121		13.5
S14	2861450	rpsN/SRA2322	61		7.1
S15	2861451	rpsO/SAR1249	89		10.4
S16	2861452	rpsP/SAR1214	91		10.1
S17	2861453	rpsQ/SAR2326	87		10
S18	2861454	rpsR/SAR0362	80	1 Ac Ala	9.4
S19	2861455	rpsS/SAR2331	92		10.4
S20	2861456	rpsT/SAR1663	83		8.8
S21	2861457	rpsU/SAR1652	58		6.8

MALDI-TOF Mass Spectrometry

The 50S precursor protein analysis was done by MALDI-TOF mass spectrometry. The sensitivity of this method makes it possible to identify the 30S and 50S ribosomal proteins based on their molecular weights. Ribosomal protein samples were prepared by acetic acid extraction and acetone precipitation as described in Methods and samples were sent for the mass spectrometry analysis to the Columbia University Core Facility, NY. Figures 19, 20, and 21 show the mass spectra of 30S subunits, 50S subunits, and the 50S precursor region proteins. Proteins were identified based on their

molecular weights predicted from the genome analysis (Holden et al. 2004). Because the post translational modifications of *S. aureus proteins* are not known, *E. coli* modifications were taken into consideration for the accurate determination of masses (Tables 4 and 5). In the 30S spectra, 17 proteins were identified. High background noise prevented identification of high molecular weight proteins S2 and S4 in the spectra. A total of twenty-five 50S proteins were identified as well. Importantly, in the 50S precursor region, 17 of 30S proteins and 16 of 50S proteins were identified. A comparison of the *E. coli* and *S. aureus* 50S precursor compositions is given in Table 9 in Discussion.

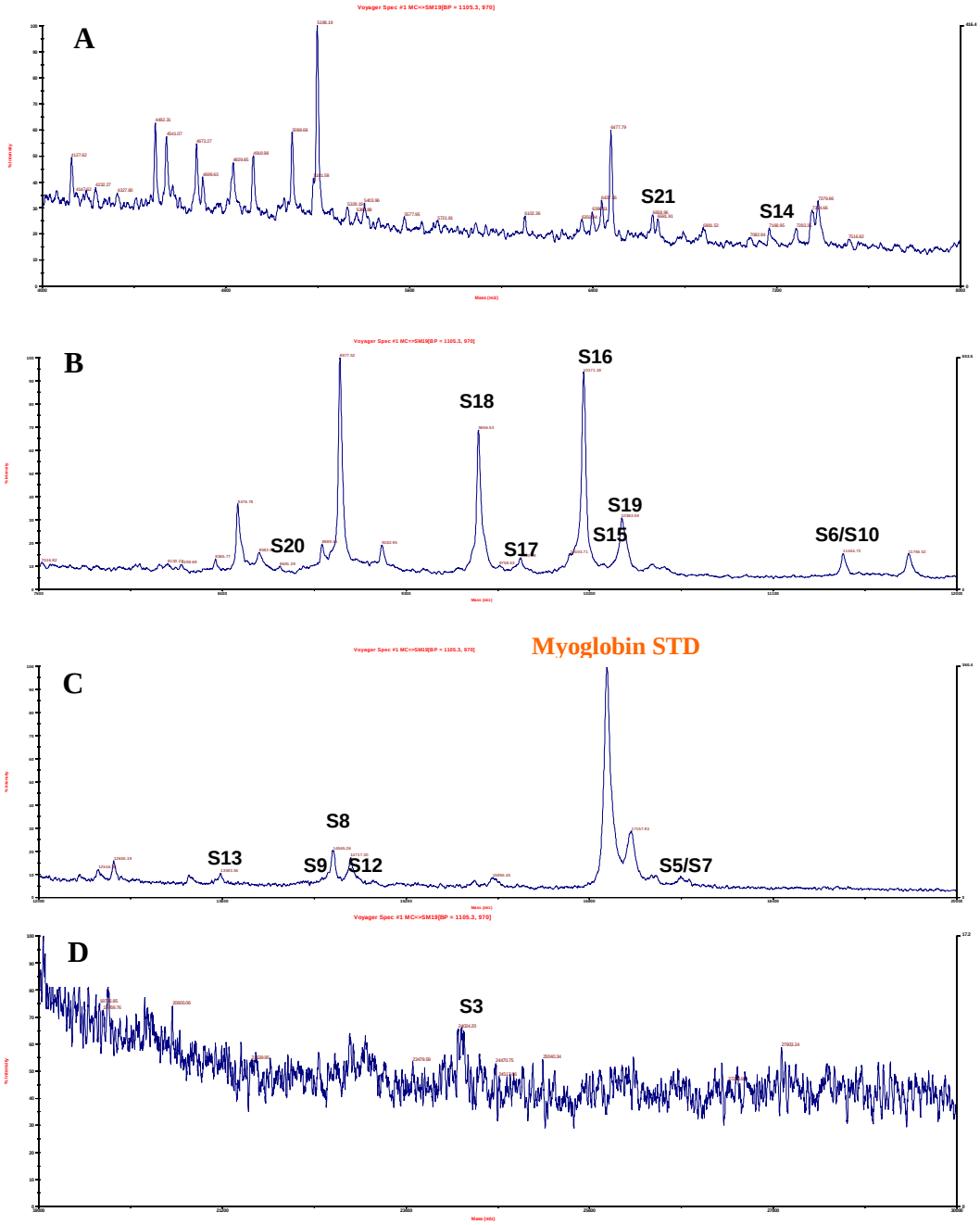

Figure 19 MALDI-TOF mass spectra for *S. aureus* 30S ribosomal proteins. Ribosomal proteins were dissolved in TFA, mixed with matrix, and spotted onto stainless steel target. Each individual spectrum represents a specific molecular weight range as indicated. A. 4000 to 8000 Da, B. 7500 to 12000 Da, C.12000 to 20000 Da, D.19000 – 30000 Da.

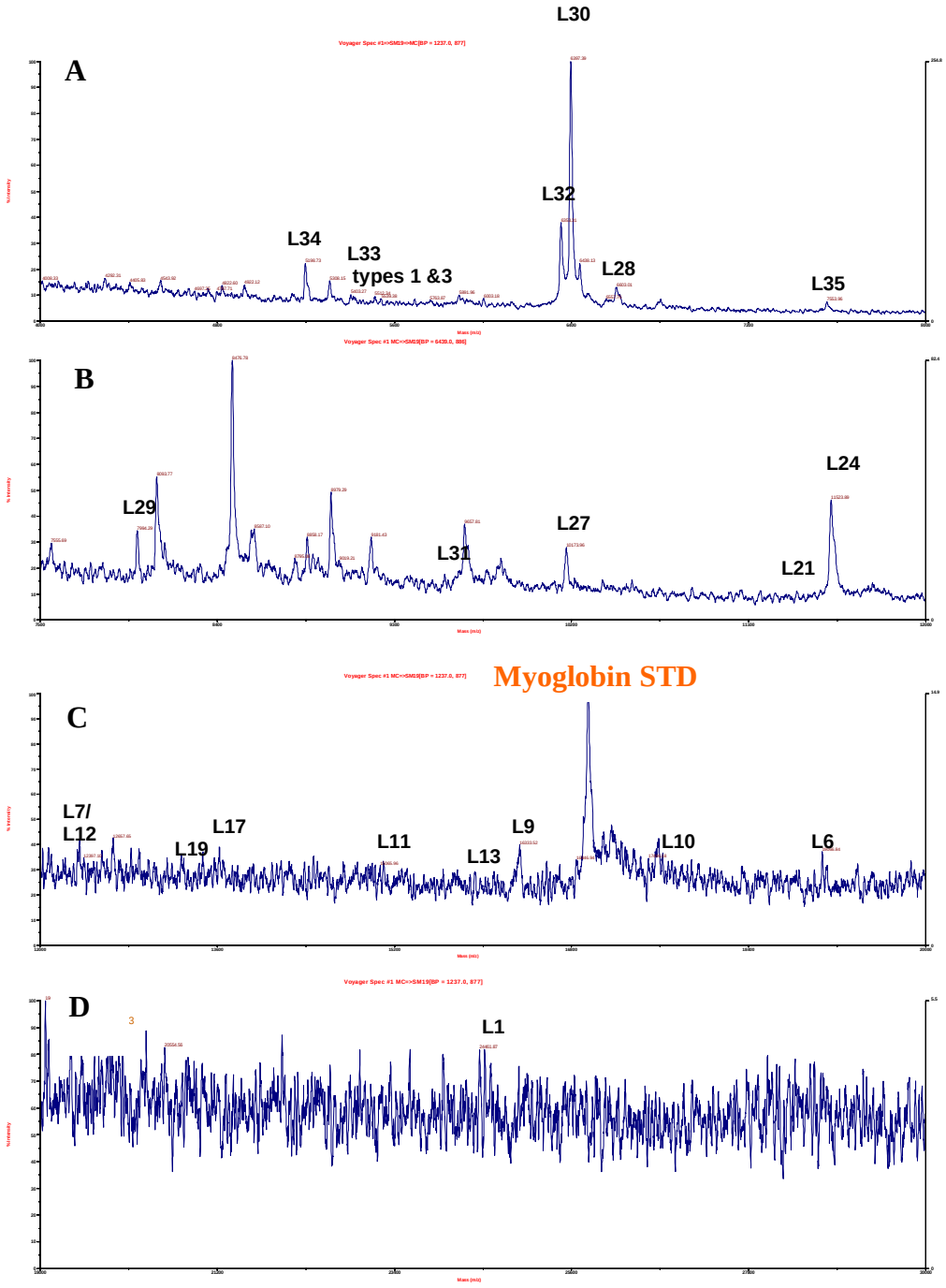

Figure 20 MALDI-TOF mass spectra for *S. aureus* 50S ribosomal proteins. Ribosomal proteins were dissolved in TFA, mixed with matrix, and spotted onto stainless steel target. Each individual spectrum represents a specific molecular weight range as indicated. A. 4000 to 8000 Da, B. 7500 to 12000 Da, C. 12000 to 20000 Da, D. 19000 to 30000 Da.

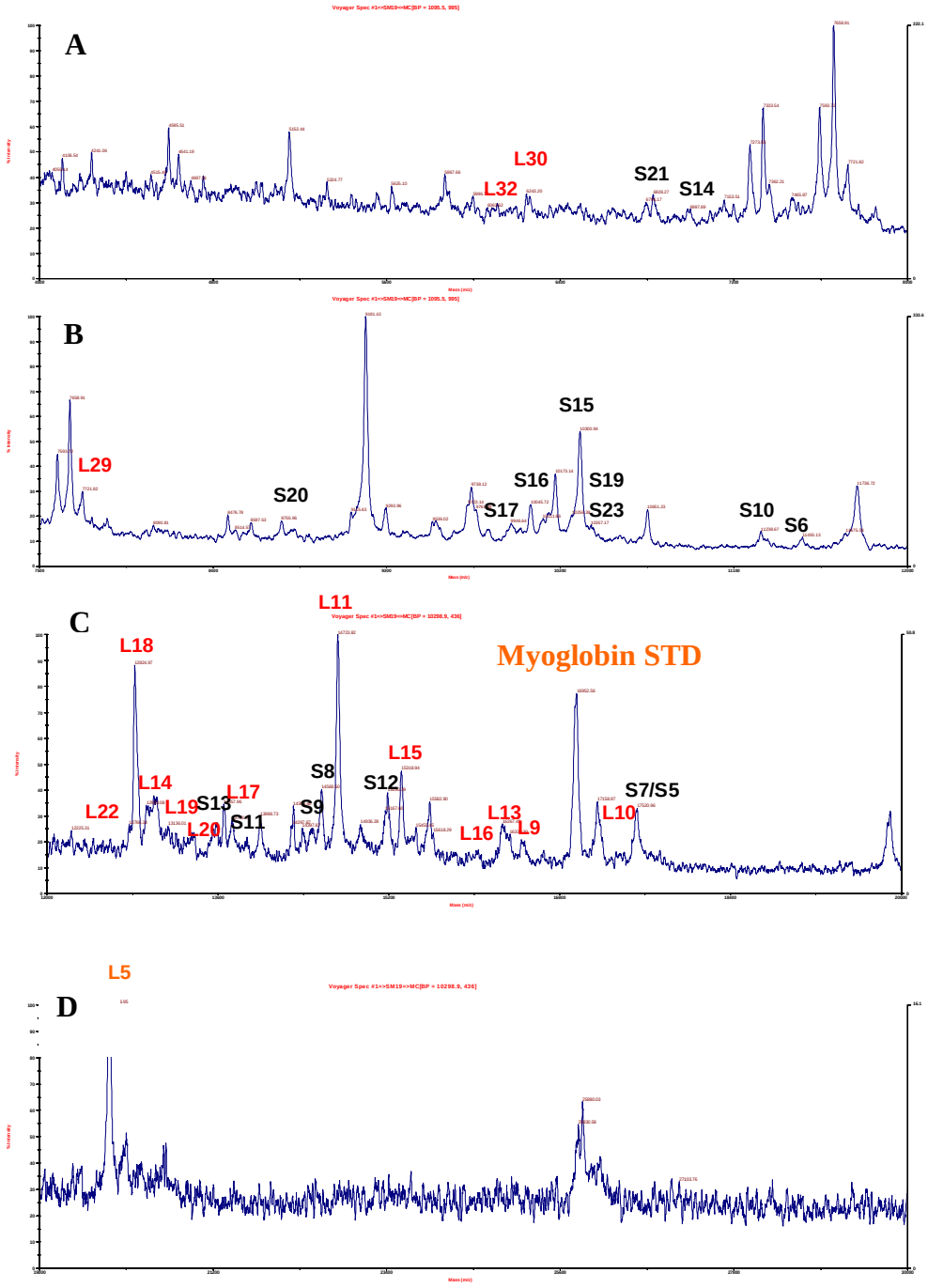

Figure 21 MALDI-TOF mass spectra for *S. aureus* ribosomal proteins from 50S precursor region of erythromycin treated cells. Ribosomal proteins were dissolved in TFA, mixed with matrix, and spotted onto stainless steel target. Each individual spectrum represents a specific molecular weight range as indicated. 30S proteins are indicated in black and 50S proteins in red. Each individual spectrum represents a specific molecular weight range as indicated. A. 4000 to 8000 Da, B. 7500 to 12000 Da, C. 12000 to 20000 Da D. 19000 to 30000 Da.

Separation of the 50S precursor particle by

hydrophobic interaction chromatography

Hydrophobic interaction chromatography has been used to separate ribosomal subunits previously (Kirillov 1978, Saruyama 1986). In the current studies, ribosomal subunits were adsorbed on to Octyl Sepharose 6B matrix and were eluted from the column with a reverse step wise concentration gradient of ammonium sulfate. Due to their inherent differences in the hydrophobicity, subunits were eluted at different concentrations of ammonium sulfate.

Subunits labeled with ^{35}S-Methionine were loaded onto the column, fractions were collected, ^{35}S-methionine was counted by liquid scintillation counting, and the elution pattern was plotted. Figure 22 indicates the elution profiles of 30S subunits and 50S subunits from control cells and the 30S and 50S precursor mixture from erythromycin treated cells. Figure 22 A shows that 30S subunits from the control cells were eluted at 1.25 M ammonium sulfate. Figure 22 B shows that the 50S subunits were eluted at 0.25 M ammonium sulfate. Importantly, Figure 22 C indicates that a major portion of the 30S and 50S mixture from the erythromycin treated cells was eluted at 0.25 M, a concentration at which the 50S subunits were eluted. This observation reinforces our previous finding that the 30S region of the erythromycin treated cells contains 50S precursor particle (Usary and Champney 2001) and that it could be separated by HIC.

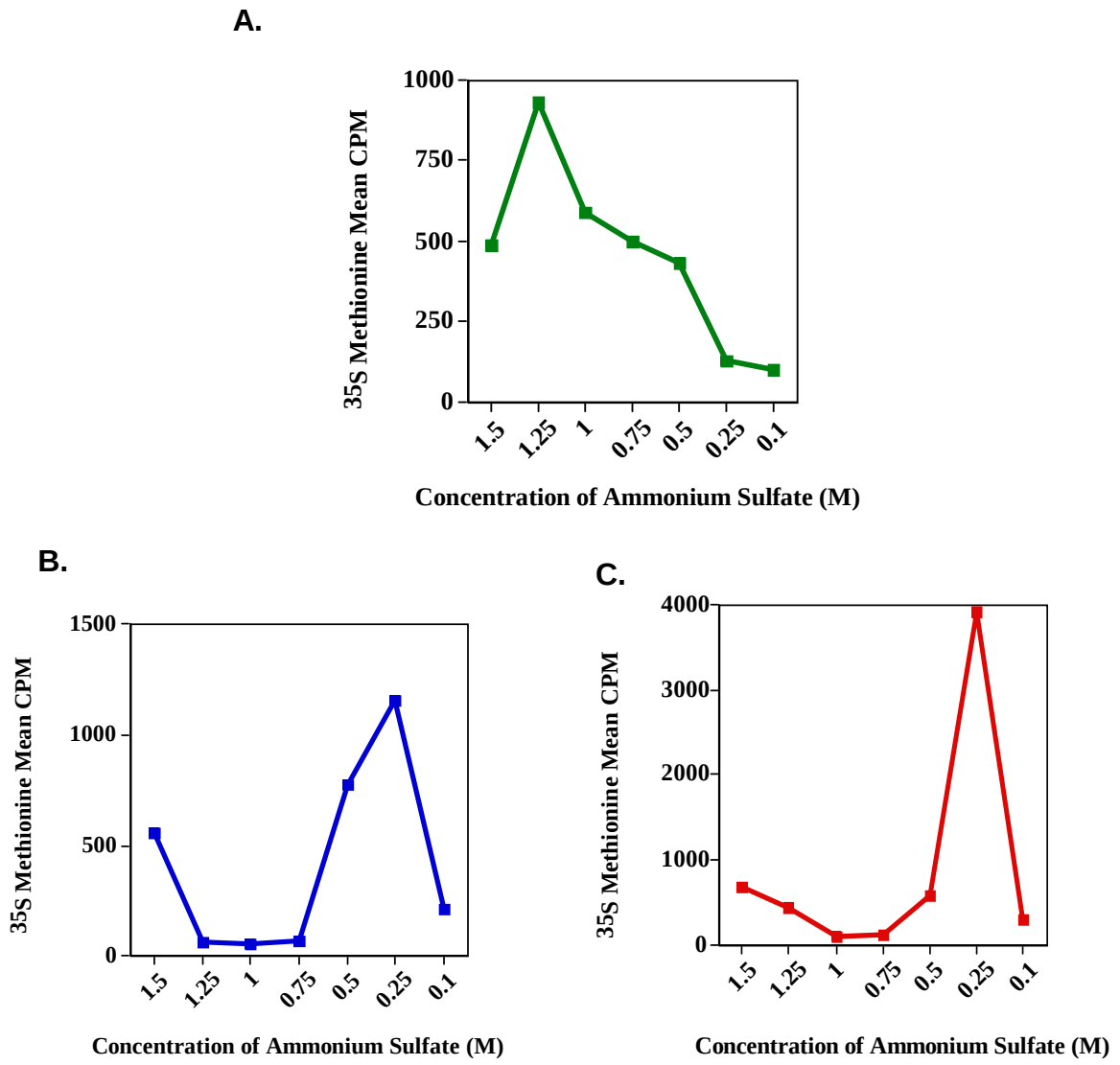

Figure 22 Ribosomal Subunit Purification by Hydrophobic Interaction Chromatography: Use of Octyl Sepharose 6B hydrophobic interaction chromatography column and step wise ammonium sulfate gradient for the purification of ^{35}S Methionine labeled (A) 30S subunits, (B) 50S subunits, and (C) 50S precursor particle. Results are the means of two experiments.

Methylation of column fractions

Fractions eluted at different ammonium sulfate concentrations from the HIC column were tested for *erm*E methyltransferase mediated ribosomal RNA methylation to establish their substrate role. The methylation assay was carried out as described for the *erm*E methyltransferase activity in the Methods section. Figure 23 demonstrates the results obtained for the *erm* methylation using ^{3}H S- adenosyl methionine as the methyl

group donor. Fractions obtained from 1.5 M- 0.75 M ammonium sulfate showed minimal methylation activity, whereas fractions eluted at 0.5 M and 0.25 M ammonium sulfate showed significant methylation activities of which the 0.25 M fractions showed the maximum methylation activity. These results further substantiate our earlier findings that a 50S precursor particle could be eluted at 0.25 M ammonium sulfate and it could act as a substrate for *erm*E methyltransferase, and fractions obtained from pure 30S or 50S subunits were not methylated by this enzyme.

Previous findings from our laboratory (Champney et al. 2003) have shown that 50S precursor particle accumulates in the 30S region of the sucrose gradients of the erythromycin treated cells. Our current findings are in agreement with the previous data and suggest a method to purify the 50S precursor from the 30S+50S precursor mixture.

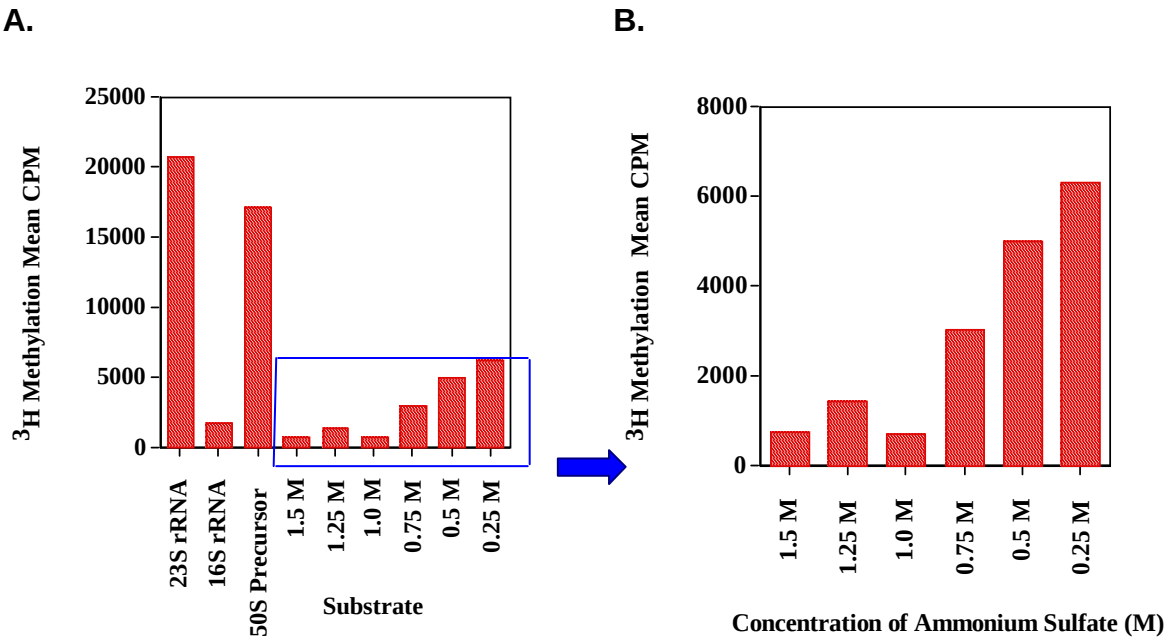

Figure 23 *erm*E methylation of HIC column fractions: Methylation was carried out as described for *erm*E methyltransferase activity with fractions obtained at different ammonium sulfate concentrations used as substrates. ^{3}H methyl RNA was counted by liquid scintillation counting and results were shown as bar graphs. A. Methylation shown along with positive (23S rRNA) and negative (16S rRNA) controls. B. Enlarged version of (A) indicated in blue box. Results are the means of two experiments.

Binding of ^{14}C Erythromycin to 50S subunits and 50S precursor particle

Studies in *E. coli* from our lab indicated that erythromycin binds to the 50S subunits and the 50S precursor particle in a 1:1 ratio (Usary & Champney 2001). In view of this finding, it was hypothesized that erythromycin will bind to both the 50S subunits and the 50S precursor particle of *S. aureus* because of the similar secondary structure of its 23S rRNA to that of *E. coli* (Garrett et al. 2000, Thompson and Dahlberg 2001). For this set of experiments the binding of ^{14}C erythromycin to the 50S precursor particle was examined with 50S subunits as positive controls (Figure 24).

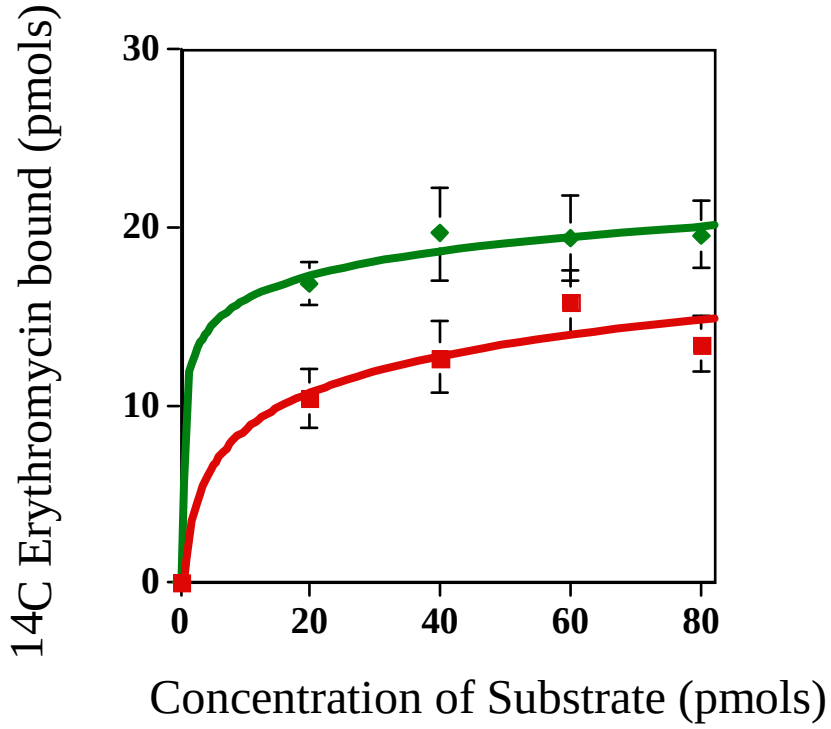

Figure 24 Binding of ^{14}C Erythromycin to the 50S subunits (♦) or to the 50S precursor particle (■). Five fold excess of ^{14}C erythromycin was added to a range of concentrations (0-80 pmols) of either 50S subunits or the 50S precursor particle. The binding assay was carried out as described in Methods. Bars indicate SEM. Results are the means of three experiments normalized with control 30S subunits.

K_M values for this binding are tabulated in Table 6. These results indicate that erythromycin does bind to the 50S precursor particle but with a lesser affinity than that of the 50S subunits.

K_M for ^{14}C Erythromycin binding to different substrates

Substrate	K_M
50S subunits	109 nM
50S Precursor Particle	154 nM

Table 6 K_M for ^{14}C Erythromycin binding to different substrates

Characterization of ermE Methyltransferase Enzyme

The *erm*E methyltransferase confers erythromycin resistance by dimethylating N-6 of A2085 in *S. aureus* 23S rRNA (Skinner 1982). It also methylates protein free 23S rRNA from *Bacillus subtilis* and *E. coli* (Skinner 1983, Vester & Douthwaite 1994). All structural elements needed for *erm*E recognition are present in domain V of 23S rRNA. In the current studies this enzyme was purified and examined for its substrate specificity in *S. aureus.* This work tests the hypothesis that the ribosomal 50S precursor particle that accumulates in erythromycin treated cells is the in vivo substrate for *erm*E methyltransferase.

For these studies, an *erm*E methyltransferase gene with a C-terminal His-tag was used that was cloned into perm60 vector for inducible expression in *E. coli* DH1. Ni-affinity chromatography was used purify this His- tagged enzyme as described in

Methods. The integrity of *erm*E methyltransferase enzyme in the eluate fractions was assessed by Western blotting and the substrate specificity was studied by methyltransferase assay.

Western Blotting of ermE Enzyme

For the *erm*E methyltransferase with C-terminal His-tag, Western blotting was done using Anti-6His mouse monoclonal antibody (Figure 25). Analysis was performed on the crude enzyme fraction obtained by the high salt wash of the perm60 ribosomes, the wash fraction of the Ni-affinity column and the eluate fraction where the enzyme is eluted from the column with 250 mM imidazole.

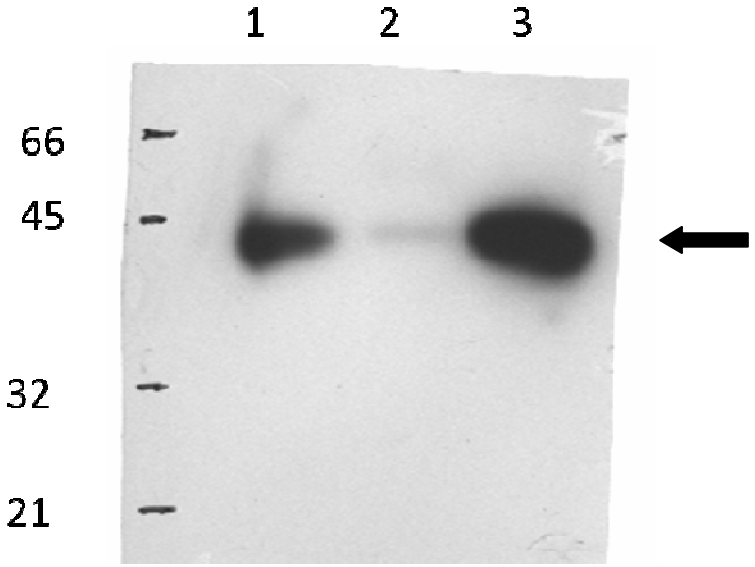

Figure 25 Western Blotting of *erm*E methyltransferase: *erm*E enzyme was purified on Ni-affinity column as described in Methods and 20µg of each fraction was subjected to 12% PAGE followed by Western blotting with anti-6His monoclonal antibody. HRP substrate on the membrane was detected by North 2 South Chemilumenescent kit and exposed to X-ray film. Lanes 1. High salt wash of the ribosome (crude enzyme fraction) 2. Wash fraction 3. Eluate fraction. Molecular weight standards are indicated in KDa. Arrow indicates *erm*E methyltransferase on the blot.

High concentrations of the enzyme were expected to be present in the crude and the eluate fractions and with efficient binding onto the Ni-affinity column it should not be eluted in the wash fraction. In agreement with our prediction, Western blotting results showed intense signal both in the crude as well as the eluate fractions. There was some non specific elution of the enzyme in the wash fraction but at very low levels. In Figure 25, enzyme was detected at the expected molecular size of 45 KDa. Importantly, there was no breakdown of the enzyme even with overloading on the gel.

ermE methyltransferase enzyme assay

The premise of this set of experiments was that a 50S precursor particle that accumulates in the 30S region of sucrose gradients of erythromycin treated cells was the in vivo substrate for *erm* E methyl transferase. The 50S precursor particle was tested as a substrate for the *erm*E methyltransferase in an in vitro methylation assay along with 23S rRNA, 16S rRNA, and 50S subunits using ^{3}H S- Adenosyl methionine as a methyl group donor. The activity of *erm*E methyltransferase was tested as a measure of enzyme mediated incorporation of ^{3}H methyl groups into the respective substrate. As evident from the Figure 26, 23 S rRNA was the best in vitro substrate as already studied (Vester and Douthwaite 1994). Apart from 23S rRNA, it was the 50S precursor particle that was methylated to a considerable extent by the enzyme. It is important to note that fully assembled 50S subunits were not methylated by the enzyme and neither were 30S subunits or 16S rRNA.

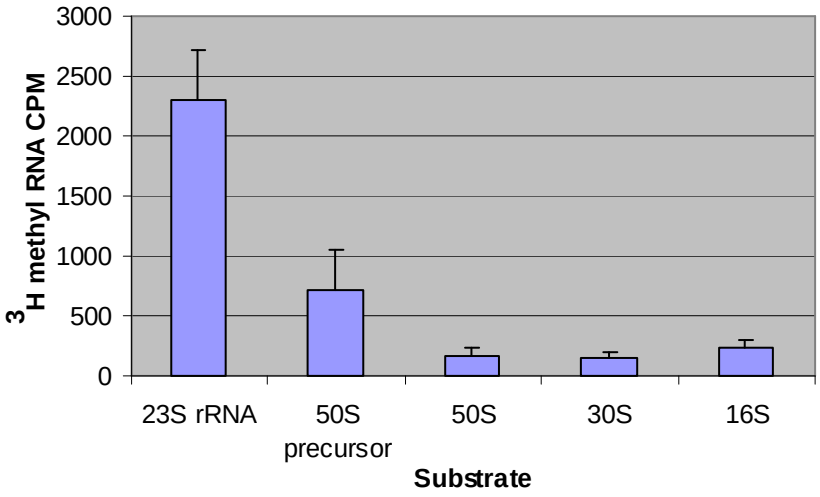

Figure 26 *erm*E methyltransferase activity assay: The assay was conducted as described in Methods with each reaction mixture containing 20 pmols of respective substrate, 3 µCi of ^{3}H SAM and 30 pmols of *erm*E methyltransferase. The activity was a measure of ^{3}H Methyl RNA formed as indicated by bar graphs. Results are the means of three experiments. Bars indicate SEM.

Inhibition of ermE methylation by MLS drugs

It was hypothesized that MLS drugs will inhibit *erm*E methyltransferase activity owing to their overlapping binding sites near the PTC. To address this hypothesis, macrolide, lincosamide, and streptogramin B drugs were tested for their ability to inhibit *erm*E methyltransferase activity. Erythromycin, lincomycin and virginiamycin S were used in these studies as representative MLS antibiotics respectively. ErmE methyltransferase activity assays were conducted as previously but in the presence of a range of concentrations of the antibiotics (Figure 27).

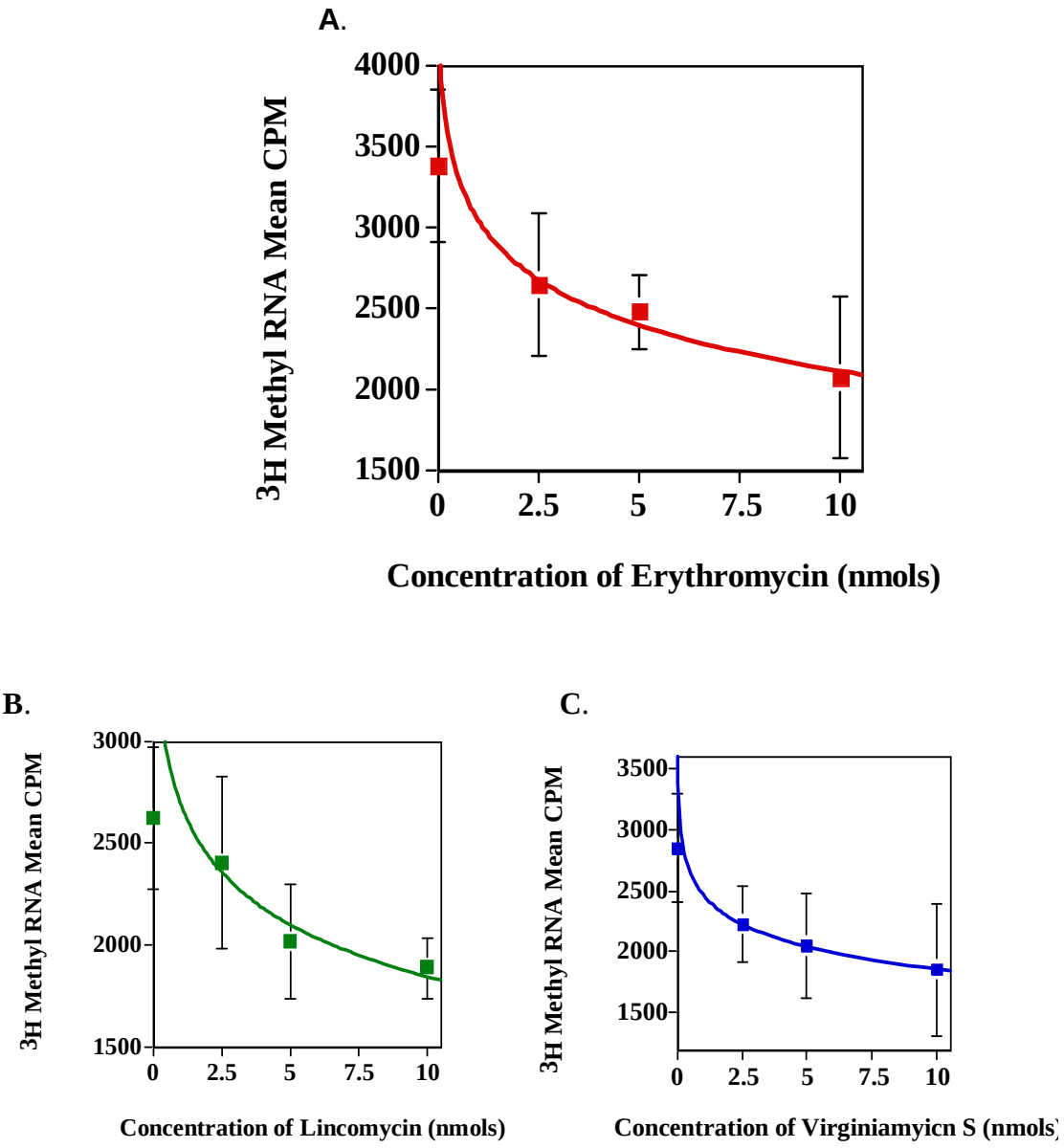

Figure 27 Concentration dependent inhibition of *erm*E methylation of 50S precursor particle by MLS antibiotics: Inhibition assays were carried out as described in Methods and inhibition of ^{3}H Methyl RNA formation was plotted as a function of the drug concentration for erythromycin, or lincomycin, or virginiamycin S. Results are the means of three experiments. Bars indicate SEM.

The results in Figure 27 indicate that all the three of the antibiotics inhibited methylation activity as a function of their concentration. Table 7 lists the inhibition

constants (K_i) for the MLS drugs. Results indicate that they have similar K_i values for *erm*E methyltransferase.

Table 7 Inhibition Constants for MLS_B antibiotics for *erm*E methyltransferase activity

Drug	**K_i (μM)**
Erythromycin	99.2
Lincomycin	132
Virginiamycin S	108

.

Competition Experiments

MLS antibiotics and *erm*E methyltransferase bind to the domain V sequences of 23S rRNA sharing a common binding site near the A2058 of *E. coli* (equivalent to A 2085 in *S. aureus*) (Skinner 1983). Earlier results from this study have shown that *erm*E methyltransferase can bind to and methylate the 50S precursor particle (Figure 26). Results in Figures 24 and 27 have also shown that MLS antibiotics can bind to the 50S precursor particle to inhibit Erm mediated methylation. Together these findings suggest that the 50S precursor particle is a substrate where there could be a potential competition between *erm*E methyltransferase and MLS antibiotics. Current experiments were designed to investigate this competition. Competition assays were performed as described with either ^{3}H SAM or ^{14}C Erythromycin. Results in Figure 28 show that methylation activity and, hence, incorporation of ^{3}H SAM into the 50S precursor particle

increased as the concentration of *erm*E methyltransferase increased even in the presence of erythromycin at 80 µM concentration, suggesting that increasing concentrations of the enzyme displaced erythromycin from its binding to the precursor. When the same assays were conducted to study binding of ^{14}C erythromycin as the enzyme concentration increased, as Figure 29 indicates, erythromycin was lost from the precursor particle.

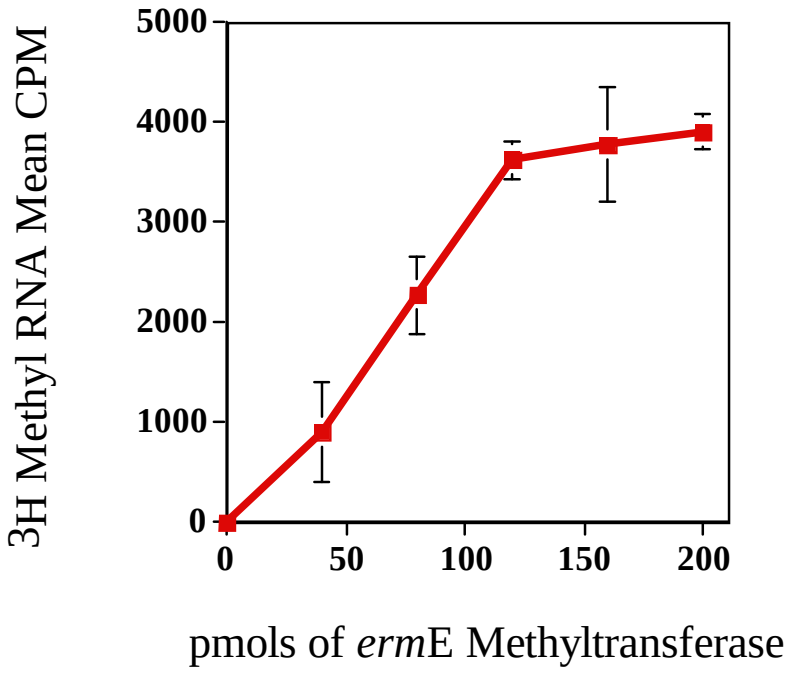

Figure 28 Competition between *erm*E methyltransferase and erythromycin: ^{3}H methylation of the 50S precursor particle with increasing *erm*E methyltransferase. Concentration of erythromycin was kept constant at 80 µM. Bars represent SEM. Results are normalized with 30S control and are the means of three experiments.

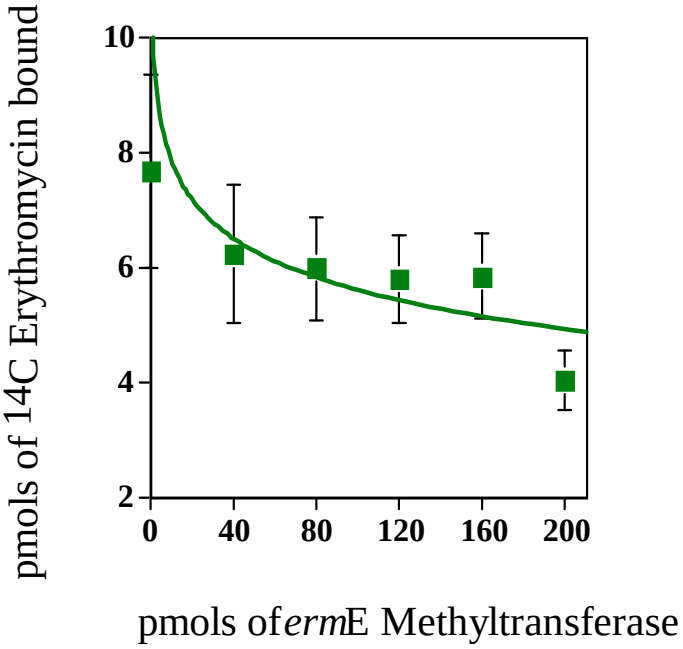

Figure 29 Competition between *erm*E methyltransferase and ^{14}C Erythromycin: Decreased ^{14}C Erythromycin binding to 50S precursor particle with increasing *erm*E methyltransferase. Bars represent SEM. Results are the means of three experiments.

. Figure 30 shows the increase in ^{3}H RNA methylation and the decrease in ^{14}C erythromycin binding simultaneously with increasing *erm*E concentrations. Results of these competition experiments indicate that the binding of either of the substrates to the 50S precursor particle finely hinges on their concentration. The Kd of *erm*E methyltransferase and the Ki erythromycin inhibition are given in Table 8.

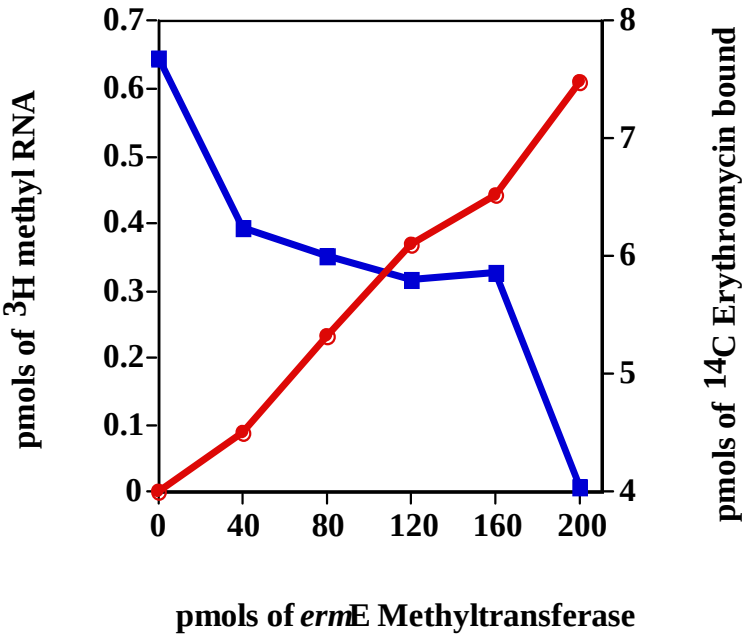

Figure 30 Competition between *erm*E methyltransferase and erythromycin for the 50S precursor particle: Increased ^{3}H methylation (●) and decreased ^{14}C erythromycin binding (■) with increasing *erm*E methyltransferase concentration.

Table 8 Comparison between Kd and Ki of ermE methyltransferase and erythromycin for the 50S precursor particle

Competitor	Kd or Ki (μM)
*erm*E methyltransferase	0.334
Erythromycin	99.2

This set of experiments confirms that *erm*E methyltransferase can actively displace erythromycin from 50S precursor particle to bring about methylation leading erythromycin resistance. A single molecule of *erm*E methyltransferase can repeat

catalysis cycles on different substrate (50S precursor) particles, whereas erythromycin binds to the substrate in a 1:1 stoichiometric fashion. This explains the low K_d of *erm* methyltransferase versus the high Ki of erythromycin. Results of these competition experiments indicate that the binding of either of the substrates to the 50S precursor particle finely hinges on their concentrations.

CHAPTER 4

DISCUSSION

Macrolides, lincosamides, and streptogramin B compounds are clinically important antibiotics that bind to the large ribosomal subunit close to the PTC (Moazed and Noller 1987, Spahn and Prescott 1996, Kirillov 1999). MLS_B resistance caused by 23S ribosomal RNA methylation is a well studied mechanism. The Erm class of methyl-transferases are responsible for this resistance phenomenon (Gaynor and Mankin 2003). Many studies have described the constitutive and inducible erythromycin resistance resulted from the action these enzymes. Much of the information about this mechanism was gained by using purified 23S rRNA as the in vitro substrate for erm methyltransferases (Uchiama 1985, Nielsen et al. 1999). Studies have shown that 50S subunits are not substrates for these enzymes (Skinner 1983, Weisblum 1995). More over, the absence of protein free 23S rRNA in the cells leaves a gap in identifying the nature of the true in vivo substrate for this class of methyltransferases. Also, not much is known about the interplay between the enzyme and MLS_B class of antibiotics at their common binding site on the PTC. The current studies were undertaken to better understand the true nature of the substrate methylated in vivo by the *erm*E methyltransferase enzyme and to understand the competition between MLS_B drugs and the enzyme for the same substrate.

Growth of S. aureus RN 1786 with erythromycin

Erythromycin is a well known protein synthesis inhibitor. Studies from our lab have shown that ribosome subunit assembly is a second important target for this macrolide antibiotic and that the stalled 50S ribosomal precursor particle accumulates in the 30S region of the sucrose gradients of lysates from the drug treated cells (Champney 2001 and 2006). The inhibitory effects of erythromycin were found to be equivalent on both the cellular process of protein synthesis and 50S subunit assembly. The formation of 30S subunits was not affected and the pre-existing 50S particles were not broken down (Champney and Burdine 1995, Chittum and Champney 1995, Champney and Burdine 1996).

In this current work, Figure 13 indicates an 82% inhibition in protein synthesis at 0.5 µg/ml erythromycin, which is in good agreement with the previous studies that showed 70% inhibition of protein synthesis at the same concentration (Champney and Tober 1998). Growth rate, cell viability, and protein synthesis (IC_{50}) were inhibited by 50% at 0.28 µg/ml, 0.31 µg/ml and 0.21 µg/ml erythromycin respectively (Table 1). Similar IC_{50}s for all the three cellular activities indicate a direct correlation between the inhibition of protein synthesis and reduction in growth rate and cell viability.

Characterization of 50S precursor particle

Experiments were done to characterize the 50S precursor particle that accumulates in the 30S region of sucrose gradients of lysates from erythromycin treated cells. Previous studies from our lab in *E. coli* showed the presence of a 50S precursor particle in the 30S region of sucrose gradients by pulse-chase labeling and antibiotic binding studies (Usary and Champney 2001). In these previous studies, the analyses

showed a decreased 50S associated rRNA in erythromycin treated cells. Identity of 23S rRNA sequences in the precursor region was confirmed by Northern hybridization using a 23S specific DNA probe. Results of these experiments showed that in control cells 75% of the 23S rRNA was present in the 50S region, whereas in drug treated cells, 40% was found in the 50S region and 35% in the 30S region. These studies are the background work for the present studies to examine the pattern of accumulation and quantitation of the 50S precursor particle amounts in *S. aureus* cells.

Characterization of rRNA by slot blot hybridization:

Characterization of the ribosomal RNA content of the 50S precursor particle was done by slot blot hybridization. The results indicated the presence of 23S ribosomal RNA in the 30S region of the erythromycin treated cells confirming the co-sedimentation of the 50S precursor particle in this region (Figure 15A). These results indicated that the proportion of 23S rRNA of this region increased with the concentration of erythromycin (Figure 15B). The percentage of 50S precursor increased from 15% to 57% as the concentration of erythromycin increased from 0.5 µg/ml to 2.0 µg/ml (Table 3). This implies that as the drug concentration increased there was an increased arrest of the 50S ribosomal subunit assembly that in turn resulted in increased accumulation of the 50S precursor particle leading to a higher proportion of 23S rRNA at elevated erythromycin concentrations in the 30S region of erythromycin treated cells.

Characterization of ribosomal proteins by two-dimensional electrophoresis:

In addition to the rRNA identification, ribosomal proteins of *S. aureus* were examined. The electrophoretic separation pattern of small and large subunit ribosomal proteins of *S. aureus* has not been studied before. Current studies used two-dimensional gel electrophoresis to analyze the ribosomal proteins of this organism (Figures 17 and18). An acidic first dimension separation at pH 5.0 and second dimensional electrophoresis in the presence of SDS were carried out to enable molecular weight determinations. In the current studies 35 50S proteins and all 21 of the 30S proteins were found in the gels. Their molecular weighs correlated with the molecular weights of *S. aureus* ribosomal proteins predicted from its genome analysis (Holden et al. 2004). Additional high molecular weight proteins that were observed in the 50S gel pattern were believed to be ribosomal binding proteins that co-sediment with the large ribosomal proteins on the sucrose gradients. These experiments are the first to study the ribosomal subunit proteins of *S. aureus*. Dekio and Jidoi analyzed 70S ribosomal proteins of *Staphylococcus aureus* Smith and *Staphylococcus epidermidis* IAM 12012 as a part of their phylogenetic studies (Dekio and Jidoi 1983). They detected 25 basic and 11 acidic proteins in the 70S subunits of *S. aureus*. In the current studies, the whole complement of 50S as well as 30S proteins was detected by two-dimensional electrophoresis.

Identification of 50S precursor proteins by MALDI-TOF mass spectrometry:

Attempts were also made to identify *S. aureus* ribosomal proteins by mass spectrometry. The protein composition of the 50S precursor particle was determined by the MALDI TOF mass spectrometry method (Figures 19-21). Mass spectrometry is a

powerful tool for the identification and characterization of proteins and peptides. Progress in the time of flight (TOF) instrumentation has improved the quality of MALDI mass spectra to the point where the masses of molecules smaller than 30,000 Da can typically be measured to an accuracy of 1 Da or better (Colby and Reilly 1994, Brown and Lennon 1995, Whittal et al. 1995). Accurate determination of the masses made it possible to identify seventeen 30S proteins and twenty-five 50S proteins by correlating with the masses predicted from the genome sequence. High noise in the 20-30 KDa region hindered the identification of high molecular weight proteins like L2 and L3. Also, in general, large proteins are often difficult to observe by MALDI-TOF in the presence of smaller proteins because of competitive ionization. Small proteins ionize readily compared to large proteins (Kaufmann 1995). Because the post translational modifications of *S. aureus* ribosomal proteins are not known, ionized species of the proteins could not be reliably identified in these spectra.

Importantly, the protein composition of the 50S precursor region of the erythromycin treated cells was analyzed by MALDI-TOF mass spectrometry. Seventeen peaks corresponding to 30S proteins were detected in this region. Significantly, sixteen 50S proteins were also detected in this region. Previously, two natural 50S precursors were studied in *E. coli*, a 32S particle, ($_{p1}$50S), and a 43S particle ($_{p2}$50S) (Homann and Nierhaus 1971, Nierhaus and Homann 1973). They both contain 23S and 5S rRNA with different proteins compositions. Previous studies in *E. coli* from our lab identified 18 large subunit ribosomal proteins in the 50S precursor particle region that accumulated in erythromycin treated cells (Usary and Champney 2001). Current studies identified 11 proteins of those 18 proteins identified in *E. coli*. They are L5, L9, L10, L11, L13, L15, L16, L17, L18, L22, and L23 (Table 9). Notably, L15 and L16 that were implicated in

erythromycin interactions of the large subunit in *E. coli* (Nierhaus 1982) were identified in the current studies also. L1-L4 identified earlier in *E. coli* could not be detected in the current studies. As mentioned earlier, difficulties in the detection of higher molecular weight proteins might have evaded their identification. Moreover, the assembly map of *S. aureus* is not available to make accurate comparisons. Information about individual proteins of *S. aureus* is needed to better understand the significance of the presence of specific proteins in the precursor region. Table 9 illustrates the composition of 50S precursor particles as described by different studies.

Table 9 Comparison of 50S precursor protein composition from different studies.

50S ribosomal Protein	*E. coli*[a] (+ ery)	*S. aureus*[b] (+ ery)
L1	+	ND
L2	+	ND
L3	+	ND
L4	+	ND
L5	+	+
L6	+	ND
L7/L12	+	−
L8	−	−
L9/L10	+	+
L11	+	+
L12	−	−
L13	+	+
L14	−	+
L15	+	+
L16	+	+
L17	+	+
L18	+	+
L19	−	+
L20	−	+
L21	−	−
L22	+	+
L23	+	+
L24	−	−
L25	+	−
L26	+	−
L27	−	−
L28	−	−
L29	−	+
L30	−	+
L31	−	−
L32	−	+
L33	−	−
L34	−	−
L35	−	−
L36	−	−

(+) Present, (−) Absent, (ND) Not Detected in the current studies.
a: Usary and Champney 2001, b: Current studies

Separartion of 50S precursor particle by HIC

All prior studies of the 50S precursor particle had been performed as a mixture with the 30S subunits of erythromycin treated cells. Previous studies had not attempted to purify the 50S precursor particle from the 30S region. HIC was previously used to isolate ribosomal subunits in *E. coli, Thermus thermophilus,* and *Halobacterium* as an alternative to zonal centrifugation (Kirillov et al. 1978, Ramakrishnan et al.1986). In these previous studies HIC was shown to be able to separate 33S and 47S particles, which are partially unfolded forms of 50S. *E. coli* 30S subunits isolated by this method were active in protein synthesis in vitro and co-migrated on sucrose gradients with subunits isolated by zonal sucrose gradient centrifugation. HIC separates subunits based on their difference in hydrophobic interaction with hydrophobic matrix material at very low concentrations of magnesium. Consequently, HIC was exploited as a method for purification of the 50S precursor particle from its mixture with the 30S subunits of erythromycin treated cells.

Results from Figure 22 showed that from the Octyl Sepharose column, 30S subunits were eluted first at a higher ammonium sulfate concentration of 1.25 M whereas 50S subunits were retained longer and eluted at a lower salt concentration of 0.25 M. An important observation was that when a 30S+50S precursor mixture was applied on to the column, a significant proportion of the sample eluted at 0.25 M ammonium sulfate, a concentration at which 50S subunits were eluted.

The eluted samples from the 30S+50S precursor mixture were further tested for their ability to be methylated by the *erm*E methyltransferase because the 50S precursor particle was shown to be a substrate for this enzyme but not the 30S subunits (Figure 26). Results of these assays revealed that the sample eluted at 0.25 M ammonium sulfate

acted as substrate for *erm*E methyltransferase, whereas the one eluting at 1.25 M did not (Figure 23). Samples eluted at other concentrations of ammonium sulfate also failed to act as substrate for *erm*E methyltransferase. These results confirm the presence of 50S precursor in the samples eluting at 0.25M.

Here the separation of 50S precursor particle by HIC was attained due to the different conformational alterations of the 30S and 50S subunits in a medium of low magnesium and high salt concentration. In this state the hydrophobic interaction of the 50S precursor particle with the hydrophobic matrix is changed. This results in its elution from the octyl sepharose column at a much lower salt concentration than the 30S subunits making the isolation of 50S precursor particle from the former feasible. These studies demonstrate HIC as a potential method of purification for the 50S precursor particle.

^{14}C Erythromycin Binding Studies

The binding of erythromycin to 50S precursor particle was studied and compared to that to the 50S subunits (Figure 24). These studies indicated that the binding affinity of erythromycin to both the 50S precursor particle and 50S subunits was similar. Binding constants for the 50S precursor particle and 50S subunits were 109 nM and 154 nM respectively and were 70 times that of the 30S subunits (K_M= 74.63 X 10^2 nM). Previous studies from our lab in *E. coli* suggested that erythromycin binds to the 50S subunits in a 1:1 ratio. The same studies also indicated binding to the 50S precursor particle to be similar to that to the 50S subunits. Current studies concur with these previous findings.

Erythromycin binding studies have shown that this drug binds to the 50S precursor particle with the same affinity as it does to the 50S ribosomal subunits. The general location of the macrolide binding site on the large ribosomal subunit has been mapped by biochemical and genetic methods previously (Ettayebi and Morgan 1985, Mozad and Noller 1987, Vester and Garrett 1987, Weisblum 1995, Hansen and Douthwaite 1999, Xiong and Mankin 1999). More details have emerged from the crystallographic studies of archaeal and bacterial large ribosomal subunits and their complexes with antibiotics (Hansen and Steitz 2000, Harms et al. 2001, Schlunzen et al. 2001).The X-ray structures indicated that ribosomal RNA constitutes the primary component of the macrolide binding site . Biochemical data revealed that macrolides including erythromycin interact mainly with the loop of helix 35 in domain V of 23S rRNA (Hansen et al. 1999, Xiong et al. 1999). Mutations or changes in posttranscriptional modifications in this rRNA region confer weak resistance to macrolides (Liu et al. 2000).

A number of nucleotide residues in the domain V of 23S rRNA interact with the macrolide molecule. Important contacts that contribute markedly to the strength of interaction of the macrolide with the ribosome are formed between the desosamine sugar moiety of erythromycin and the rRNA. The desosamine sugar of erythromycin and other related fourteen-membered macrolides form hydrogen bonds with nucleotide residues A2058 and 2059 (*E. coli* numbering). The nucleotide at position 2057 may also be involved in hydrogen bonding with the C5 of the desosamine sugar (Schlunzen et al. 2001) of erythromycin. In the case of 15 or 16 membered ring macrolides, the same nucleotide may establish hydrophobic bonding with the lactone ring (Hansen et al. 2002). In addition, the desosamine sugar can potentially interact with the backbone phosphate

oxygen of G2505. Interaction of the lactone ring accounts for more than 25% of the free energy of binding of macrolides (Garga-Ramos et al. 2002).

Ketolides are the most recently introduced generation of modified macrolides. They contain a 11, 12- carbamate ring where macrolides have free hydroxyl groups. The 11-OH and 12-OH lactone hydroxyls of erythromycin and related drugs form a hydrogen bond with O4 of U2609 whereas the carbamate ring of ketolides forms hydrogen bonds with this group. But this interaction is more important for ketolides than for erythromycin group of macrolides because a mutation of U2609 confers resistance to ketolides but not to macrolides (Garga-Ramos et al. 2002).

ermE methyltransferase Studies

In the present work, the true in vivo substrate for the ermE methyltransferase enzyme was probed. Previous studies showed the 50S precursor particle as an important substrate for *erm*C methyltransferase enzyme in *S. aureus* (Champney et al. 2003). These studies have also shown that fully assembled 50S subunits were not methylated as others have found (Skinner et al. 1983, Weisblum 1995).This finding was consistent with a model that predicted the accumulation of a stalled 50S precursor particle in erythromycin treated cells. Relief from inhibition and continued particle synthesis can occur only by precursor methylation that reduces erythromycin binding to 50S subunits.

The same studies proposed a model to account for this activity. In wild-type organisms, erythromycin stalls the 50S particle formation, and cellular ribonucleases promote the degradation of the rRNA and turnover of the incomplete precursor particle

(Silvers and Champney 2005). In *S. aureus* RN 4220 cells with an inducible *erm* gene erythromycin also stalled the assembly of the nascent subunit (Champney, Chittum, and Tober 2003). However, in this case the stalled precursor particle would be a substrate for the *erm* methyltransferase enzyme. Methylation of the 23S rRNA in the precursor particle relieves the assembly inhibition, permitting the synthesis of methylated particles that are resistant to the inhibitory effects of the antibiotic. This assembly sequence explains why mature 50S subunits are not methyltransferase substrates.

Purification and detection of ermE methyltransferase

The *erm*E methyltransferase was purified from a cloned vector $_p$erm60 with a C-terminal histidine tag. Comparison studies with an untagged *erm*E have shown that the HIS_6 sequence tag does not detectably affect the ability of the enzyme to methylate RNA substrates (Douthwaite et.al. 1998). In these studies, SDS polyacrylamide gel electrophoresis was used to assess the purity of the enzyme. In the current studies after its purification on Ni-affinity chromatography column and elution with 250 mM imidazole, *erm*E methyltrasnferase was detected by Western blotting using an anti His_6 monoclonal antibody (Figure 25).

The cloned methyltransferase (calculated molecular weight 43.6 KDa) migrated slightly faster than the ovalbumin marker protein (45 KDa) on the gel. As expected in the crude and eluate fractions, a strong signal was obtained at the corresponding molecular weight of the enzyme. There was some non-specific elution of the enzyme in the absence of imidazole in the wash fraction but this signal was minimal. Importantly, there was no breakdown of the enzyme as suggested by the single band in the eluate fraction. Thus

Western blotting provides evidence for the purification of an integral *erm*E methyltransferase.

ermE methyltransferase Activity Assay

The current studies with *erm*E methyltransferase are an extension to the previous studies with the *erm*C methyltransferase (Champney et al. 2003). Moreover, those studies were conducted with a crude extract of *erm*C methyltransferase as a preliminary probe into the true nature of in vivo *erm* substrate. In the current studies, assays were carried out with the purified eluate fraction of the Ni-affinity column. 23S rRNA, a 50S precursor particle, 50S subunits, 30S subunits, and 16S rRNA were all tested as substrates. Figure 26 indicated that purified 23S rRNA was the functional substrate for the enzyme as also shown by other studies (Skinner et al 1983, Weisblum 1995). It was also observed that the 50S precursor particle showed considerable methylation. Significantly, fully assembled 50S subunits failed to act as substrates although they contain 23S rRNA and the full complement of 50S proteins. However, 30S subunits and 16S rRNA were not methylated by the enzyme as well.

These findings essentially confirm the results obtained earlier with *erm*C. Based on these observations, it was hypothesized that the true in vivo substrate for *erm*E methyltransferase is the 50S subunit precursor particle that sediments along with the 30S subunits on the sucrose gradients of the lysates from erythromycin treated *S. aureus* cells. It was also proposed that this precursor particle is composed of 23S rRNA and a subset of 50S ribosomal proteins essential for *erm* methylation.

The *erm*E methyltransferase assay results (Figure 26) are consistent with this hypothesis, and the results showed that maximum level of methylation occurred with

23S rRNA as the substrate and that the 50S precursor particle that showed a considerable degree of methylation. Poor methylation activities were observed with 50S and 30S ribosomal subunits and 16S rRNA. Significantly, the absence of protein free 23S rRNA in the cells and the failure of fully assembled 50S subunits to act as substrate further substantiate the hypothesis that the 50S precursor particle as the true in vivo substrate for *erm*E methyltransferase.

These results draw attention to the conformation of 23S rRNA needed for *erm*E recognition. Enzyme activity depends both on the primary and secondary structure around the methylation site (Kovalic 1995, Nielsen et al. 1999, Villsen et al. 1999). The requirement for high enzyme fidelity in recognizing a single target amongst an array of rRNA nucleotides reveals the uniqueness of this rRNA region and thus sequence specificity. The nucleotides at positions 1055 and 2058 to 2061 are conserved over 95% (Villsen et al. 1999).

Studies of O'Farrell and Rife on 16S rRNA methylation using kasugamycin resistance showed that in *E. coli* a 30S ribosomal assembly intermediate serves as a substrate for KsgA, a dimethyltransferase, strongly support our findings (Thammana 1974, O'Farrell et al. 2006). In *E. coli*, kasugamycin resistance results from a mutation at the *ksg*A locus due to the lack of the methylase activity (Helser 1971, Helser 1972, Zimmerman 1973). Ksg encodes for an adenosine dimethyltransferase that dimethylates A1518 and A1519 in the 16S rRNA of *E. coli*. It was shown that neither 16S rRNA nor 30S subunits in a translationally active state were substrates for the enzyme in vitro (Thammana 1974, Desai and Rife 2006). In recent studies it was shown that KsgA recognizes a complicated substrate. Methylation occurs during 30S assembly, where a particle containing 16S rRNA along with 8 core proteins is the

methylation substrate. Although KsgA can bind to naked 16S rRNA, it remained enzymatically inactive until a partially matured 30S subunit was assembled. The in vivo minimal substrate required 16S RNA plus the ribosomal proteins S4, S6, S8, S11, S15, S16, S17, and S18, suggesting that dimethylation of A1518 and A1519 might occur during a specific point during ribosome assembly.

The above conclusions were supported by numerous structural data of the 30S subunit in the active and inactive conformations. In the crystal structure of *Thermus thermophilus* 30S subunit in which the 30S was in an active conformation, A1518 and A1519 were well buried into the grove of helix 44 and, therefore, sequestered from KsgA. However, conversion to the inactive state exposed the same two nucleotides to the solvent.

Slot blot hybridization (Figure 15) identified the presence of 23S rRNA in the 50S precursor particle and sixteen large ribosomal proteins were found in this region by MALDI-TOF mass spectrometric analysis (Figure 21). Together, these results propose this 50S precursor as a particle analogous to the one identified earlier in *E. coli* (Usary and Champney 2001). It has all the components needed for erythromycin binding as well as for *erm* methylation, although the significance of individual proteins still needs to be elucidated. In the absence of a protein free 23S rRNA in the cells, these findings strongly support the current hypothesis of 50S ribosomal precursor particle being an in vivo substrate for *erm*E methyltransferase.

Inhibition of ermE methylation by MLS_B antibiotics:

MLS_B drugs, represented by erythromycin, lincomyin, and virginiamycin S, share a

common binding site on the 50S subunits and hence on the 50S precursor particle. The peptidyltransferase domain on the 50S subunit is a common target for the MLS_B antibiotics that includes the erm methylation site A2085 in the helix V of 23S rRNA. MLS_B drugs cause steric hindrance to the binding of *erm* methyltransferase and hence could act as inhibitors of the latter's activity. Data from Figure 27 showed that this prediction was true. MLS_B drugs inhibited *erm*E methyltransferase activity in a concentration dependent manner. Inhibition constants of all the three drugs were found to be similar.

Competition Assays

In the inhibition curves, it was seen that the erm methylation activity was inhibited with the concentration of the MLS drugs. This is expected when there is a direct competition in the binding of both these agents to the 50S precursor particle. The protein free 23S rRNA and the 50S precursor particle containing 23S rRNA with a subset of 50S proteins are substrates for *erm*E methyltransferase. The methylation site A2085 is accessible for the enzyme action, whereas erythromycin binds to the 50S precursor particle and 50S subunits where the PTC in domain V is available for erythromycin binding. This transition suggests that 50S precursor particle, in the middle of the assembly sequence, has the all the sequence and conformation features needed for the binding of both the enzyme and the drug (Figure 31).

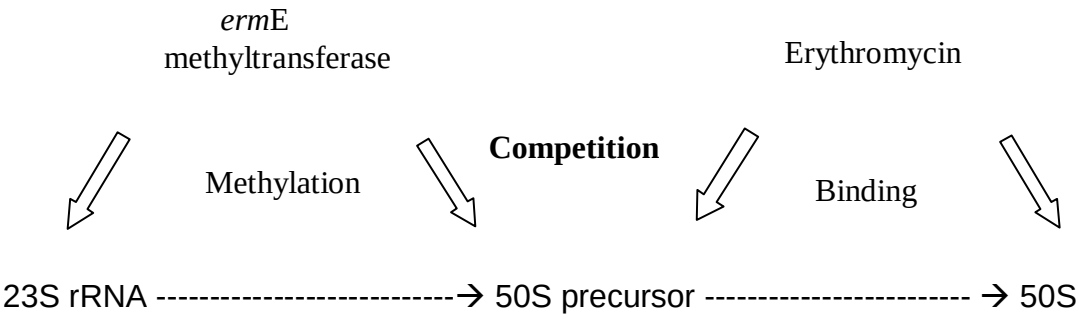

Figure 31 Model showing the interaction of erythromycin and *erm*E methyltransferase with the 50S precursor particle.

Another set of competition experiments is shown in Figures 28 and 29. The results of Figure 28 indicate that at increasing concentrations, *erm*E methyltransferase displaced erythromycin from the 50S precursor particle resulting in increasing methylation levels. Similar assays examining the binding of ^{14}C erythromycin binding showed decreased erythromycin binding with increasing concentrations of *erm*E methyltransferase (Figure 29). Competition experiments indicated that the association constant (K_M) of *erm*E methyltransferase is 330 fold higher than the inhibition constant (K_i) of erythromycin suggesting the requirement for a higher concentration of the drug to prevail over methylase.

Hence, competition between these two substrates for the 50S precursor particle is an obligatory outcome when both are present. The fine tuning of the competition depends on the kinetics of their binding. Erythromycin binds to the 50S precursor particle in a 1:1 ratio resulting in every stalled precursor particle affectively having one drug molecule bound whereas a single *erm*E methyltransferase molecule can repeat catalysis cycles to methylate different 50S precursor particles making them MLS resistant. Thus, the stoichiometry of erythromycin binding and the catalysis of *erm* methylase are two very

important factors that determine which one binds to the 50S precursor particle.

Competition between erythromycin and *erm*E methyltransferase at the PTC was studied for the first time. These in vitro kinetic studies yielded a better understanding of the interaction of the antibiotic and the enzyme at their binding site. Studies of this nature provide important clues about the interplay between the drug and the enzyme in the erm producing strains leading to erythromycin resistance.

Inhibitors of *erm* methyltransferase have been studied to sensitize bacteria that are resistant to erythromycin in vivo and in vitro. In this regard, it is of interest to note that S- Adenosyl-L-homocysteine, the metabolic product of S-adenosyl-L-methionine after the methyl group transfer, is a naturally occurring inhibitor of erm methyltransferase with a K_i of 40 µM. Fesik and coworkers (Katz 1999) have screened a small library of heterocyclic compounds for their anti erm activity. Hannesian and Sgarbi designed mimics of S-adenosyl-L-homocysteine as potential inhibitors of erm methyltransferases (Hanessian and Sgarbi 2000). Sinefungin is another general inhibitor of methyltransferases, which is a natural nucleoside occurring in *Streptpmyces griseolus*. Chemically, sinefungin is S-adenosyl ornithine (Goldman and Kadam 1989).

In view of the limited clinical success of these inhibitors, it is important to further understand the true cellular target for *erm* methylase and to know if the enzyme can actively displace bound erythromycin from the precursor substrate. Current studies yielded information needed for a more rational approach for antibiotic development. and therapy strategies against the clinically important pathogen *S. aureus*.

REFERENCES

Amabile-Cuevas CF, Cardenas-Garcia M, and Ludgar M. (2003). Antibiotic Resistance. *American Scientist, 83,* 320-329.

Anderson RM. (1999). The pandemic of antibiotic resistance. *Nature Med., 5,147-149*

Anderson S and Kurland CG.(1987). Elongating ribosomes in vivo is refractory to erythromycin. *Biochimie., 69,* 901-904.

Arthur M and Andermont A. (1987). Distribution of erythromycin esterases and rRNA methylase in members of the family Enterobacteriaceae highly resistant to erythromycin. *Antimicrob Agents Chemother. 31*, 404-409.

Ban N,Nissen P, Hansen J, Moore PB, and Steitz TA. (2000). The complete atomic structure of the large ribosomal subunit at 2.4 Å resolution. *Science, 289,* 905-920.

Bernabeu, and Lake.JA. (1982). Nascent polypeptide chains emerge form the exit domain of the large ribosomal subunit: immune mapping of the nascent chain. *Proc.Natl.Acad.Sci.USA, 79,* 3111-3115.

Brown RS. and Lennon JJ. (1995). Mass resolution improvement by incorporation of pulsed ion extraction in a matrix-assiststed laser desorption/ ionization linear time-of-flight mass spectrometer. *Anal.Chem, 69,* 1998-2003.

Champney WS. (2003). Bacterial ribosomal subunit synthesis is an antibiotic target. *Curr Topics Med.Chem, 3*, 929-947.

Champney WS. and Tober CL. (1998). Inhibition of translation and 50S subunit formation in *Staphylococcus aureus* cells by eleven different ketolide

antibiotics. *Curr Microbiol, 37,* 418-425.

Champney WS. and Burdine R. (1995). Macrolide antibiotics inhibit 50S ribosomal subunit assembly in *Bacillus subtilis* and *Staphylococcus aureus*. *Antimicrob Agents Chemother., 39,* 2141-2144.

Champney WS. and Burdine R. (1996). 50S ribosomal subunit synthesis and translation are equivalent targets for erythromycin inhibition in *Staphylococcus aureus. Antimicrob Agents Chemother. 40,* 1301-1303.

Champney WS, Chittum HS, and Tober CL. (2003). A 50S ribosomal subunit precursor particle is a substarte for the ErmC methyl transferase in *Staphylococcus aureus* cells. *Curr Microbiol., 46,* 453-460.

Champney WS. (2001). Bacterial ribosomal subunit synthesis: A novel antibiotic target. *Current Drug Targets-Infectious Disorders. 1,* 19-36.

Champney WS, Tober CL. and Burdine R. (1998). A comparison of inhibition of translation and 50S ribosomal subunit formation in Staphylococcus aureus cells by nine different macrolide antibiotics. *Current Microbio., 37*, 412-417.

Champney WS. (2006). The other target for ribosomal antibiotics: Inhibition of bacterial ribosomal subunit formation. *Infectious Disorders-Drug Targets. 6,* 1-14.

Chittum HS. and Champney WS. (1994). Ribosomal protein gene sequence changes in erythromycin-resistant mutants of *Escherichia coli*. *J.Bacteriol*. *176,* 6192-6198.

Cohen ML. (1994). Antimicrobial Resistance:Prognosis for public health. *Trends Microbiol., 2,* 422-425.

Colby SM, KingTB, and Reilly JP. (1994). *Rapid Commun.Mass Spectrom. 8,* 865-868.

Cundliffe E. (1990). Recognition sites for antibiotics within rRNA. Ed: Hill WE, Dahlberg A, Garrett RA, Moore PB, Schlessinger D, Warner JR. The Ribosome: Structure, Function and Evolution. *ASM, Washington DC,*

Chu TWD, Platter JJ, and Katz L. (1996). New directions in antibacterial research. *J. Med. Chem., 39,* 3854-3874.

Dekio S. and Jidoi J. (1983). Characterization of ribosomal proteins from *Staphylococcus* and *Micrococcus* by two-dimensional gel electrophoresis. *The Journal of Dermatology, 10*, 267-274.

DiGiambattista M. and Vanuffel P. (1986). Antagonistic interactions of macrolides and synergimycins on bacterial ribosomes. *J.Antimicrob Chemother. 10,* 307-315.

Douthwaite SR. (1992). Interaction of the antibiotics clindamycin and lincomycin with *Escherischia coli* ribosomes. *Nucleic Acids Res, 20*, 4717-4720.

Dubnau D. (1985). Induction of erm C requires translation of the leader peptide. *EMBO J, 4,* 533-537.

Duval J. (1985). Evolution and epidemiology of MLS resistance. *J.Antimicrob Chemother., 16,* 137-148.

Ettayebi M, Prasad SM, and Morgan EA. (1985). Chloramphenicol-erythromycin resistance mutations in a 23S rRNA gene of *Escherichia coli. J.Bacteriol.162,* 551-557.

Fenn JB, Mann M, Meng CK, Wong SF, and Whitehouse CM. (1989). Electrospray

ionization for mass spectrometry of large biomoleules. *Science, 26,* 64-71.

Frank J, Penczek P, Li Y, Srivastava S, Verschoor A, Radermacher M, Grassucci R, Lata RK, Agarwal RK, and Zhu J. (1995). A model of protein synthesis based on cryo-electron microscopy of the *E. coli* ribosome. *Nature, 376,* 441-444.

Gabashvili IS, Valle M, Grassucci R, Worbs M, Wahls MC, Dahlberg AE, Frank J. and Gregory ST. (2001). The polypeptide system in the ribosome and its gating in erythromycin resistant mutants of L4 and L22. *EMBO J., 8.* 181-188.

Gale EF, Cundliff E, Reynolds PE, Richmond MH, and Waring MJ. (1981). The molecular basis of antibiotic action. *John Wiley & Sons, New York, NY*.

Garga-Ramos G, Xiong L, Zhong P, and Mankin A. (2002). Binding site of macrolide antibiotics on the ribosome: New resistance mutation identifies a specific interaction of ketolides with rRNA. *J. Bacteriol., 183,* 319-323.

Garrett RA, Douthwaite SR, Liljas A, Matheson AT, Moore PB, and Noller HF. (2000). The ribosome structure, function, antibiotics and cellular interactions. *American Society for Microbiology, Washington, DC, Symposium,*

Gaynor M. and Mankin AS. (2003). Macrolide antibiotics: Binding site, mechanism of action, resistance. *Current Topics in Medicinal Chemistry, 3,* 463-469.

Goldman RC and Kadam SK. (1989). Binding of novel macrolide structures to macrolides-lincosamides-streptogramin B resistant ribosomes inhibit protein synthesis and bacterial growth. *Antimicrob Agents Chemother., 33,* 1058-1066.

Gregory ST. and Dahlberg AE. (1999). Erythromycin resistance mutations in ribosomal proteins L22 and L4 perturb the higher order structure of 23S

ribosomal RNA. *Jour .of Mol. Biol., 289,* 827-834.

Gryczan T, Grandi G, Hahn J, Grandi J. and D.Dubnau. (1980). Conformational alteration of mRNA structure and the posttranscriptional regulation of erythromycin-induced drug resistance. *Nucleic Acids Res., 8,* 6081-6097.

Hajduk PJ, Dinges J, Schkeryantz JM, Janowick D, Katz L, and Fesik A. (1999). Novel inhibitors of Erm methyltransferases from NMR and parallel synthesis. *J.Med. Chem., 42,* 3852-3859.

Hansen JL, Ippolito JA, Ban N, Nissen P, Moore P B, and Steitz TA. (2002). The structures of four macrolide antibiotics bound to the large ribosomal subunit. *Mol. Cell, 10,* 117-126.

Hansen LH, Mauvais P, and Douthwaite SR. (1999). The macrolide-ketolide antibiotic binding site is formed by structures in domain II and domain V of 23S ribosomal RNA. *Mol.Microbiol. 31,* 623-631.

Harms J, Schlunzen F, Zarivach R, Bashan A, and Gat S. (2001). High resolution structure of the large ribosomal subunit from a mesophilic eubacterium. *Cell,* 107, 679-688.

Hanessian S. and Sgarbi PWM. (2000). Design and synthesis of mimics of S-Adenosyl-L-homocysteine as potential inhibitors of erythromycin methyltransferases. *Bioorganic & Medicinal Chemistry Letters, 10,* 433-437.

Helser TL, Davies JE, and Dahlberg JE. (1971). Change in methylation of 16S ribosomal RNA associated with mutation to kasugamycin resistance in *Escherichia coli. Nature New Boil., 233*, 12-14.

Helser TL, Davies JE, and Dahlberg JE. (1972). Mechanism of kasugamycin resistance in *Escherichia coli*. *Nature New Boil., 235*, 6-9.

Holden MT, Titball RW, Peacok SJ, Cerdeno-Terraga AM, Atkins T, Crossman LC, Pitt T, Churcher C, Mungall K, and Bentley SD et al. (2004). Complete genomes of two clinical *Staphylococcus aureus* strains. Evidence for the rapid evolution of virulence and drug resistance. *Proc.Natl.Acad.Sci.USA,101, 9786-9791.*

Homann HE. and Nierhaus KH. (1971). Ribosomal proteins. Protein composition of biosynthetic precursors and artificial subparticles from ribosomal subunits in Escherischia coli. *Eur.J.Biochem,20,* 249-257.

Horinouchi S. and Weisblum B. (2006). Posttranscriptional Modification of mRNA Conformation: Mechanism that regulates erythromycin-induced resistance. *Proc.Natl.Acad.Sci.USA, 77,*7079-7083.

Jett B, Huycke M, Gilmore MH, and Atter K. (1997). Simplified agar plate method for quantifying viable bacteria. *Bio Techniques, 23,* 648-650.

Karas M, Buchmann D, Bahr U, and Hillenkamp F. (1987). Matrix-assisted laser desorption of nonvolatile compounds. *Int.J.Mass.Spectrom.Ion Processes, 78,* 53-68.

Kaufman R. (1995). Matrix assisted laser desorption ionization (MALDI) mass spectrometry: a novel analytical tool in molecular biology and biotechnology. *J. Biotechnol. 41,* 155-175.

Kirillov S, Porse BT, Vester B, Wooley P, and Garrett RA. (1997). Movement of the 3' end of t-RNA through the peptidyl transferase center and its inhibition by antibiotics. *FEBS Lett., 406,* 223-233.

Kirillov S, Porse BT, and Garrett RA. (1999). Peptidyl transferase antibiotics perturb the relative positioning of the 3'-terminal adenosine of P/P - site bound tRNA and 23S rRNA in the ribosome. *RNA, 5,* 1003-1011.

Kirillov S, Makhno VI, Peshin NN, and Semenkov YP. (1978). Separation of ribosomes of *Escherichia coli* by sepharose chromatography using reverse salt gradient. *Nucleic Acids Res.,* 4305-4315.

Koepsel RR, Murray RW, Rosenblum WD, and Khan SA. (1985), Purification of pT181-encoded repC protein required for the initiation of plasmid replication. *J.Biol.Chem, 260,* 8571-8577.

Kovalic D, Giannattasio RB, and Weisblum B.(1995). Methylation of minimalist 23S rRNA sequence in vitro by Erm SF (TlrA) N- methyltransferase. *Biochemistry, 4,* 15838-15844.

Lai CJ. and Weisblum B. (1971), Altered methylation of ribosomal RNA in an erythromycin resistant strain of *Staphylococcus aureus,* P*roc.Natl.Acad.Sci.USA, 68*, 856-860.

Lampson BC, Von David W, and Parisi JT. (1986). Novel mechanism for plasmid-mediated erythromycin resistance from *Staphylococcus epidermidis. Antimicrob Agents Chemother., 30,* 653-658.

Leclercq R. and Courvalin P. (1991).Intrinsic and unusual resistance to macrolides, lincosamides, and streptogramin antibiotics in bacteria. *Antimicrob Agents Chemother., 35,*1273-1276.

Leclercq R. and Courvalin P. (2002). Resistance to macrolides and related antibiotics in *Streptococcus pneumoniae, Antimicrob Agents Chemother 46,* 2727-2746.

Leung DYM, Meissner HC, Fulton DR, Murray DL, Kotzin BL, and Schlievert PM. (1993). Toxic-shock syndrome toxin secreting *Staphyloccocus aureus* in Kawasaki syndrome. *Lancet, 342*, 1385-1388.

Liebold WB. (1986). Structure, function and genetics of ribosomes. *Springer-Verlag, New York.* 326-361.

Liu M, KirpekarF, Van Wezel GP, and Douthwaite,SR. (2000). The tylosin resistance gene tlrB of *Streptomyces fradiae* encodes a methyltransferase that targets G748 in 23S rRNA. *Mol.Microbiol.37,* 811-820.

Locksley RM, Cohen ML, and Quinn TC. (1982). Multiply antibiotic-resistant *Staphylococcus aureus*: Introduction, transmission and evolution of nosocomial infection. *Ann Intern Med, 97,* 317.

Madzar JJ, Michael S, Cozzone AJ, and Rebound JP. (1979). A method to identify individual proteins in four different two-dimensional electrophoresis systems: Application to *Escherichia coli* ribosomal proteins. *Anal. Biochem. 92,* 174-182.

Mao JCH. and Puttermann M. (1979). The intermolecular complex of erythromycin and ribosome. *J.Mol.Biol., 44,* 347-361.

Mazzei T, Mini E, Novelli A, and Periti P.(1993). Chemistry and mode of action of macrolides. *J.Antimicrob.Chemother., 31*, 1-9.

Marana MC, Moreira B, Boyle-Vavra S, and Daum RS. (`997). Antimicrobial resistance in *Staphylococci, Infectious Disease Clinics of North America, 11,* 813-848.

Melish ME, Parsonett J, and Marchette N.(1994). Kawasaki syndrome is not caused by toxic shock syndrome toxin-1 (TSST-1)+ S*taphylococci*,

Pediatr.Res., 135, 187A.

Miller JH. (1972). Experiments in molecular genetics. *Cold Spring Harbor Laboratory, Cold Spring Harbor, NY.*

Moazed D and Noller HF. (1987). Chloramphenicol, erythromycin, carbomycin and vernamycin B protect overlapping sites in the peptidyl transferase region of 23S rRNA. *Biochimie, 69,* 879-884.

Nielsen AK, Dothwaite SR, and Vester B.(1999). Negative in vitro selection identifies the rRNA recognition site for erm E methyltransearse. *RNA, 5,* 1034-1041.

Nierhaus K, Bordash K, and Homann HE. (1973). In vivo assembly of *Escherischia coli* ribosomal proteins. *J.Mol.Biol, 74,* 587-597.

Nierhaus K. (1982). Structure, assembly and function of ribosomes. *Curr.Topics.Microbiol.Immunol., 97,* 81-155.

Odom OW, Picking WD, Tsalkova T, and Hardesty B. (1991). The synthesis of polyphenylalanine on ribosomes to which erythromycin is bound. *Eur.J.Biochem., 198,* 713-722.

O'Farell, HC, Pulicherla N, Desai PM, and Rife JP. (2006). Recognition of a complex substrate by the KsgA/Dim 1 family of enzymes has been conserved throughout evolution. *RNA, 12,* 725-733.

Omura S. (1984). Macrolide Antibiotics, *Academic Press Inc. Orlando, FL.*

Pestka S. (1972). Studies on transfer ribonuclei acid-ribosome complexes. Effect of antibiotics on peptidyl puromycin synthesis on polyribosomes from *Escherichia coli*. *J.Biol.Chem, 247*, 4669-4678.

Rubinstein E. (1994). Reviewing the antibiotic miracle. *Science, 264,* 360-393.

Ramakrishnan V, Graziano V, and Capel MS.(1986). A role for proteins S3 and S14 in the 30S ribosomal subunit. *J.Biol.Chem., 264,* 15049-15052.

Saruyama H. (1986). Isolation of ribosomal subunits from an extremely halophilic archaebacterium *Halobacterium halobium* by hydrophobic interaction chromatography. *Anal.Biochem., 159*, 12-16.

Schlunzen F, Zarivach R, Harms J, Bashan A, Tocilj A, Albrecht R, Yonath A, and Franceschi F. (2001). Structural basis for the interaction of antibiotics with the peptidyl transferase center in eubacteria. *Nature 413,* 814-821.

Skinner R. and Cundliffe E. (1982). Dimethylation of adenine and the resistance of *Streptomyces erytherus* to erythromycin., *J.Gen.Microbiol, 128,* 2411-2416.

Skinner R, Cundliffe E, and Schmidt FJ. (1983). Site of action of a ribosomal RNA methylase responsible for resistance to erythromycin and other antibiotics. *J.Biol.Chem, 258,* 12702-12706.

Silvers JA. and Champney WS. (2005). Accumulation and turnover of 23S ribosomal RNA in azithromycin-treated ribonuclease mutants strains of *Escherichia coli. Arch Microbiol., 184,* 66-77.

Spahn CM. and Prescott CD. (1996). Throwing a spanner in the works: antibiotics and the translation apparatus. *J.Mol.Med, 74,* 723-739.

Tauman SB, Jones NR, Young FE, and Corcoran JW. (1966). Sensitivity and resistance to erythromycin in *Bacillus subtilis* 168: The Ribosomal binding of erythromycin and chloramphenicol. *Biochim.Biophys.Acta. 123,* 438-440.

Takashima H. (2003). Structural consideration of macrolide antibiotics in relation to the ribosomal interaction and drug design. *Current Topics in Medicinal Chemistry, 3,* 991-999.

Thompson RL, Cabezudo I, and Wenzel RP.(1982). Epidemiology of nosocomial infections caused by methicillin resistant *Staphylococcus aureus. Ann Intern Med, 97,* 309.

Thompson J, Taprich WE, Munger C, and Dahlberg AE. (2001). *Staphylococcus aureus* domain V functions in Escherichia coli ribosomes provided a conserved interaction with domain IV is restored. *RNA, 7,* 1076-1083.

Thammana P. (1974). Methylation of 16S rRNA during ribosome assembly in vitro. *Nature 254,* 682-686.

Uchiyama H. and Weisblum B.(1985). N-Methyl transferase of *Streptomyces erythreus* that confers resistance to macrolide-lincosamide-streptogramin B antibiotics: amino acid sequence and its homology to cognate R-factor enzymes from pathogenic bacilli and cocci. *Gene 38,* 103-110.

Usary J. and Champney WS. (2001). Erythromycin inhibition of 50S ribosomal subunit formation in *Escherichia coli* cells. *Mol.Microbiol, 40,* 951-962.

Vazquez D. (1979). Inhibitors of protein synthesis. *Springer-Verlag:Berlin, Heidelberg, New York.*

Vester B. and Douthwaite SR.(2001). Macrolide resistance conferred by base substitutions in 23S rRNA. *Antimicrob Agents Chemother., 45,* 1-12.

Vester B. and Douthwaite SR. (1994). Domain V of 23S rRNA contains all structural elements necessary for recognition by ErmE methyltransferase. *J.Bacteriol, 176,* 6999-7004.

Vester B. and Garrett RA. (1987). A plasmid coded and site-directed mutation in *Escherichia coli* 23S rRNA that confers resistance to erythromycin: implications for the mechanism of action of erythromycin. *Biochimie, 69*, 891-900.

Vester B,.Neilsen AK, Hansen LH, and Douthwaite SR.(1998). Erm E Methyl Transferase recognition elements in RNA substrates. *J.Mol.Biol., 282*, 255-264.

Villsen ID, Vester B, and Douthwaite SR. (1999). Erm E methyltranferase recognizes features of the primary and secondary structure in a motif within domain V of 23S rRNA. *J.Mol.Biol., 19,* 365-374.

Voss A. and Doebelling B. (1995). The world-aide prevalence of methicillin-resistant *Staphylococcus aureus*. *Int.J.Antimicrob.Agents, 5,* 101-106.

Weisblum B, Graham MY, Gryczan T, and Dubnau D. (1979). Plasmid copy number control: isolation and characterization of high-copy-number mutants of plasmid pE194. *J.Bacteriol.137,* 635-643.

Weisblum B. (1998). Macrolide resistance. *Drug Resist.Updates, 1*. 29-41.

Weisblum B. (1985). Inducible resistance to macrolides,lincosamides and streptogramins type B antibiotcs; The resistance phenotype, its biological diversity, and structural elements that regulate expression. A review. *J..Antimicrobial Chemotherapy, 16 Suppl*. 63-90.

Weisblum B. (1995). Erythromycin resistance by ribosome modification. *Antimicrob Agents Chemother., 39,* 577-585.

Whittal RM. and Li. L. (1995). High-resolution matrix-assisted linear

desorption/ionization in a linear time-of-flight mass spectrometer. *Anal.Chem., 67,* 1950-19545.

Wilcox SK, Cavery GS, and Pearson JD. (2001). Single ribosomal protein mutations in antibiotic-resistant bacteria analyzed by mass-spectrometry. *Antimicrob Agents Chemother., 45,* 3046-3055.

Whittmann HG, Tanaka K, Tamaki M, Apirion D, Rosen L, Takata R, Dekio S, and Otaka E. (1973). Biochemical and genetic studies on two different types of erythromycin resistant mutants of *Escherichia coli* with altered ribosomal proteins. *Mol.Gen.Genet.,127,* 175-189.

Wiley PFL, .Baczynskyj L, Dolak LA, Ciandella JI, and Marshall VP. (1987), Enzymatic phosphorylation of macrolide antibiotics. *J.Antibiot, 40,* 195-201.

Xiong L, Shah S, Mauvais P, and Mankin AS. (1999), A ketolide resistance mutation in domain II of 23S rRNA reveals proximity of hairpin 35 to the peptidyl transferase center. *Mol.Microbiol., 31*, 633-639.

Zimmerman RA. and Ikeya Y. (1974). Alteration of ribosomal protein S4 by mutation linked to kasugamycin resistance in *Escherichia coli*. *Proc.Natl.Acad.Sci.USA, 70,* 71-75.

APPENDIX

ABBREVIATIONS

PTC…… … Peptidyl Transferase Center

IDV…… Integration Density Value

Ec…….. Escherichia coli

Dr…….. Deinococcus radiodurans

Erm…….. Erythromycin Resistance Methylase

rRNA…… Ribosomal RNA

MLS_B…… Macrolide, Lincosamide, Streptogramin B

30S…….. Small subunit of ribosome

50S …….. Large subunit of ribosome

SAS buffer…… *S. aureus* subunit buffer

R buffer …… Ribosome buffer

IC_{50}…… 50% Inhibition Concentration

TSB…… Tryptic Soy Broth

SDS…… Sodium dodecyl sulfate

PMSF…….. Phenylmethylsulfonylfluoride

TCA…… Trichloroacetic acid

SAM…… S-Adenosyl Methionine

PAGE…….. Polyacrylamide Gel Electrophoresis

MES…… 2-[N-Morpholino]ethane sulfonic acid

TE…… Tris EDTA buffer

TEMED…… Tetramethylethylenediamine

APS…… Ammonium per sulfate

VITA

INDIRA DEVI POKKUNURI

Personal Data:	Date of Birth: June 4, 1971 Place of Birth: India Marital Status: Married
Education:	Public Schools, Kakinada, India B.Sc, Biology, Andhra University, Visakhapatnam, AP, India 1991 M.Sc, Biochemistry, Andhra University, Visakhapatnam, AP, India 1994 Ph.D., Biomedical Sciences, East Tennessee State University, Johnson City, TN 2007
Professional Experience:	Junior Research Fellow, University of Hyderabad, Hyderabad, India, 1995- 1997 Lecturer, V.S. Lakshmi Women's Degree College, Kakinada, India, 1997-2001 Graduate Assistant, East Tennessee State University, Johnson City, TN 2001-2007
Publications:	Indira Pokkunuri and W. Scott Champney. "Competition Between Erythromycin and *erm*E methyltransferase Enzyme for a 50S Precursor Particle in *Staphylococcus aureus*". (Manuscript in Preparation)